Biochimica et Biophysica Acta 1853 (2015) 1294–1315

Contents lists available at ScienceDirect

Biochimica et Biophysica Acta

journal homepage: www.elsevier.com/locate/bbamcr

Review

Structure–function analysis of NEET proteins uncovers their role as key regulators of iron and ROS homeostasis in health and disease ☆

Sagi Tamir [a,1], Mark L. Paddock [b,1], Merav Darash-Yahana-Baram [a], Sarah H. Holt [c], Yang Sung Sohn [a], Lily Agranat [a], Dorit Michaeli [a], Jason T. Stofleth [b], Colin H. Lipper [b], Faruck Morcos [d,e,f,g], Ioav Z. Cabantchik [a], Jose' N. Onuchic [d,e,f,g], Patricia A. Jennings [b], Ron Mittler [c], Rachel Nechushtai [a,*]

[a] The Alexander Silberman Life Science Institute and the Wolfson Centre for Applied Structural Biology, Hebrew University of Jerusalem, Edmond J. Safra Campus at Givat Ram, Jerusalem 91904, Israel
[b] Department of Chemistry and Biochemistry, University of California at San Diego, La Jolla, CA 92093, USA
[c] Department of Biology, University of North Texas, Denton, TX 76203, USA
[d] Center for Theoretical Biological Physics, Rice University, Houston, TX 77050, USA
[e] Department of Physics and Astronomy, Rice University, Houston, TX 77050, USA
[f] Department of Chemistry, Rice University, Houston, TX 77050, USA
[g] Department of Biochemistry and Cell Biology, Rice University, Houston, TX 77050, USA

ARTICLE INFO

Article history:
Received 4 July 2014
Received in revised form 1 October 2014
Accepted 16 October 2014
Available online 23 October 2014

Keywords:
Mitochondria
2Fe–2S cluster
Cluster donor/acceptor protein
Wolfram Syndrome 2
Homeostasis
Cancer
Obesity and diabetes

ABSTRACT

A novel family of 2Fe–2S proteins, the NEET family, was discovered during the last decade in numerous organisms, including archea, bacteria, algae, plant and human; suggesting an evolutionary-conserved function, potentially mediated by their CDGSH Iron–Sulfur Domain. In human, three NEET members encoded by the *CISD1–3* genes were identified. The structures of CISD1 (mitoNEET, mNT), CISD2 (NAF-1), and the plant At-NEET uncovered a homodimer with a unique "NEET fold", as well as two distinct domains: a beta-cap and a 2Fe–2S cluster-binding domain. The 2Fe–2S clusters of NEET proteins were found to be coordinated by a novel 3Cys:1His structure that is relatively labile compared to other 2Fe–2S proteins and is the reason of the NEETs' clusters could be transferred to apo-acceptor protein(s) or mitochondria. Positioned at the protein surface, the NEET's 2Fe–2S's coordinating His is exposed to protonation upon changes in its environment, potentially suggesting a sensing function for this residue. Studies in different model systems demonstrated a role for NAF-1 and mNT in the regulation of cellular iron, calcium and ROS homeostasis, and uncovered a key role for NEET proteins in critical processes, such as cancer cell proliferation and tumor growth, lipid and glucose homeostasis in obesity and diabetes, control of autophagy, longevity in mice, and senescence in plants. Abnormal regulation of NEET proteins was consequently found to result in multiple health conditions, and aberrant splicing of NAF-1 was found to be a causative of the neurological genetic disorder Wolfram Syndrome 2. Here we review the discovery of NEET proteins, their structural, biochemical and biophysical characterization, and their most recent structure–function analyses. We additionally highlight future avenues of research focused on NEET proteins and propose an essential role for NEETs in health and disease. This article is part of a Special Issue entitled: Fe/S proteins: Analysis, structure, function, biogenesis and diseases.

© 2014 Elsevier B.V. All rights reserved.

1. Preface: Fe–S proteins — major players in health and disease

Performing a wide-range of biological processes essential to sustain life, iron–sulfur proteins are highly conserved throughout evolution. Most commonly, they harbor 2Fe–2S and/or 4Fe–4S clusters, which partially mediate these proteins' multiple functions [1,2]. The redox potential of these Fe–S clusters varies from −500 mV to +300 mV (SHE), making them excellent electron donors/acceptors capable of driving different fundamental chemical reactions involved in processes such as respiration, photosynthesis and nitrogen fixation [3]. Indeed in these essential processes the most well established function of Fe–S containing proteins is to serve as electron transfer (ET) proteins. However, in the last decade new evidence has emerged showing that the Fe–S clusters of numerous Fe–S proteins have additional functions, such as sensing of iron or oxygen, as well as substrate binding/catalysis and gene expression regulation [2,3].

The biogenesis of iron–sulfur clusters is a multi-step process involving complex protein machinery [3–6]. In eukaryotes, more than 17

☆ This article is part of a Special Issue entitled: Fe/S proteins: Analysis, structure, function, biogenesis and diseases.

* Corresponding author.
E-mail address: rachel@mail.huji.ac.il (R. Nechushtai).

[1] Equal contribution.

http://dx.doi.org/10.1016/j.bbamcr.2014.10.014
0167-4889/© 2014 Elsevier B.V. All rights reserved.

proteins are involved in Fe–S cluster biogenesis [7], localizing to both the cytosol, mitochondria [8], and chloroplasts. Fe–S biogenesis proteins facilitate the assembly of the cluster as well as its transfer to inactivate Fe–S holo-proteins [5,6]. In recent years, an increasing number of genetic-based human diseases have been attributed to mutations in Fe–S proteins, many of which are proteins shown to be associated with dysfunction of the Fe–S cluster biogenesis pathway. Examples include Friedreich's ataxia, glutaredoxin 5-deficient sideroblastic anemia, ISCU myopathy, and ABCB7 sideroblastic anemia/ataxia syndrome [9–13]. Among the genetic diseases directly associated with a gene encoding a 2Fe–2S protein is Wolfram Syndrome 2 (WFS-2) [14]. This neurological disorder results from a mutation in the *CISD2* gene leading to loss of the 2Fe–2S cluster of the NAF-1 (nutrient-deprivation autophagy factor-1, synonyms: ERIS, Miner1, CISD2, Noxp70) protein, a member of the recently discovered NEET protein family [8,9,15,16].

2. The discovery of NEET proteins and their initial characterization

2.1. The NEET family of proteins

MitoNEET (mNT), the founding member of the NEET family of proteins, was discovered as a mitochondrial protein that binds the anti-type 2 diabetes drug, pioglitazone [17]. With the completion of a draft human genome sequence it became evident that mNT in humans belongs to a family of three mNT-like human proteins (18). The initial names given to the mNT paralogs were Miner1 and Miner2 meaning *mi*to*NE*ET *r*elated *1* and *mi*to*NE*ET *r*elated *2*, respectively. Miner1 has also been named ERIS, Noxp70 and NAF-1 due to its association with disease, neural development and autophagy [14,19]. We here refer to the second member of the NEET family as NAF-1. Upon identifying the three human NEET family members, it became evident that all three members share a 39 amino acid stretch called the CDGSH domain [18] . The three human NEET proteins are encoded by the *CISD1*, *CISD2* and *CISD3* genes in which CISD stands for *C*DGSH *I*ron–*S*ulfur *D*omain. Within the CDGSH domain is a 16 amino acid stretch that was later shown in the mNT crystal structure to contain the four ligands of the Fe–S cluster (Fig. 1) [20]. Using UV–vis and MS analysis, we demonstrated that mNT harbored a labile and redox active 2Fe–2S cluster [21]. As the UV–vis spectra of NAF-1 and Miner2 are very similar to that of mNT, we deduced that they similarly contain 2Fe–2S clusters (Fig. 1). This was later confirmed for NAF-1 by the determination of its crystal structure [21]. It should be noted here that Miner2 encoded by the *CISD3* gene is the least characterized member of this gene family and thus it is described in less detail in this review.

MitoNEET was found to be localized to the mitochondria as originally predicted [17]. In addition, it was shown to be tethered to the outer mitochondrial membrane (OMM) with the major part of the protein, including its C-terminal domain, located in the cytosol [18]. In contrast, GFP-fused NAF-1 was shown to be more diffused in its localization [18]. Its distribution was more indicative of association with the endoplasmic reticulum (ER); one of its earlier names was ERIS meaning *ER Iron–Sulfur* protein [14]. Other studies, however, showed its association with mitochondria [22]. Most recently, in a detailed subcellular localization study, NAF-1 was shown to be localized to the mitochondria-associated membrane (MAM) that connects the ER to the OMM [16], perhaps unifying the previous disparate localization studies. Miner2 was shown to localize (predominantly) to the mitochondria, although details about its submitochondrial localization are not yet known [18]. Thus, all three members of the human NEET family are located on, or in proximity to, the mitochondrial membrane with mNT and NAF-1 containing a single transmembrane helix for anchoring.

2.2. Identifying the 2Fe–2S cluster of NEET proteins

Identification and characterization of the ion metals that comprise the NEET proteins' CDGSH domain required high amounts of purified protein. In order to achieve that, the transmembrane N-terminal helix was removed and a His-tag was added to mNT [20], and NAF-1 [21]. When purified from *Escherichia coli* cells, the recombinant His-tagged truncated NEET proteins were red in color. As this color is indicative of iron, the metal composition was measured. The isolated mNT protein contained more iron than any other metals [18]. Using the isolated protein, we were able to obtain UV–vis spectra and utilize more biophysical techniques to characterize the Fe state of this protein. The UV–vis

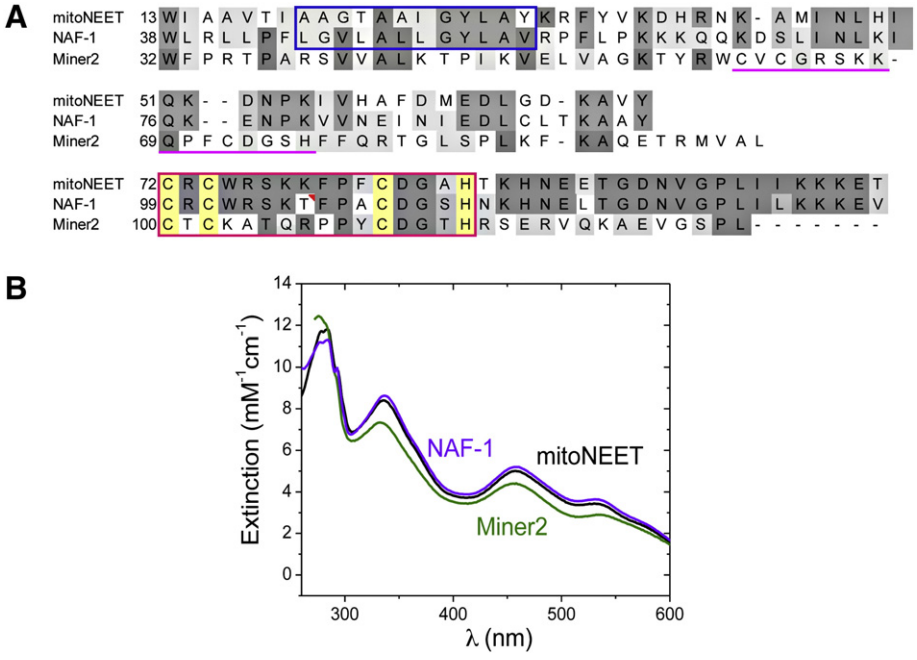

Fig. 1. Human NEET protein alignments and UV–vis spectra. (A) Amino acids conserved in humans are shown in gray. Amino acids that coordinate to the 2Fe–2S clusters are shown in yellow. The 16 amino acid cluster binding domains are boxed in magenta. Note that Miner2 has a repeat of the 16 amino acid 2Fe–2S cluster binding domain, underlined in pink. The transmembrane domains of mitoNEET and NAF-1 are highlighted by a blue box. (B) UV–vis spectra of mitoNEET, NAF-1 and Miner2. Note the similarities of the peak positions in the visible region which are ligand to metal charge transfer bands reflecting the presence of the same type of Fe–S clusters and the similarity of their coordinations.

spectra were distinct and showed absorbance peaks that were similar to that of known iron–sulfur containing proteins, such as ferredoxin and Rieske (see below), indicative of intact iron–sulfur clusters in the samples. Furthermore, reduction with a strong reducing agent, dithionite, showed the expected spectral changes associated with the reduction of an iron–sulfur cluster [20]. However, these observations alone did not provide definitive evidence for the type of iron–sulfur cluster, *e.g.* 2Fe–2S or 4Fe–4S. The finding that the Fe–S cluster of mNT dissociated at lower pH, allowed the determination of the mass of the protein prior to and following the loss of its iron–sulfur cluster. Mass spectroscopy (MS) allowed us to easily distinguish between holo- and apo-mNT making this measurement less susceptible to the purity of the starting material. A mixture of apo- and holo-mNT would therefore appear as two separate peaks with distinct masses. The mass difference between the apo- and holo-mitoNEET showed unambiguously that the cluster in mNT is a 2Fe–2S cluster. These findings suggested that the 2Fe–2S cluster of NEET proteins could be used for electron reduction/transfer in a process that could be modulated by changing pH [20].

Replacement of the His87 with Gln (H87Q mutant) eliminated the cluster and replacement of the His87 with Cys (H87C mutant) altered the UV–vis spectrum and stabilized the 2Fe–2S cluster establishing that His 87 is most likely the non-Cys ligand of the cluster (Fig. 2). In the H87C mutant, the absorption peak positions in the visible range of the spectrum were slightly shifted from the native as an expected consequence of changing the ligation to the 2Fe–2S cluster (Fig. 2A); the Vis absorption peaks are due to ligand to metal charge-transfer interactions. His114 of NAF-1 is the equivalent of His87 of mNT and more recent studies indicated similar optical absorbance changes and labile properties of NAF-1 and its H114C mutant (Fig. 2B) and [21,23].

As the lability of the 2Fe–2S clusters of NEET proteins is quite sensitive to their environment, cluster stability measurements have become one of the first measures of interactions of NEET proteins with small molecules and/or other proteins, as well as for the effect of mutations on the cluster stability and dynamics (Fig. 2).

2.3. Structure of NEET proteins

2.3.1. Structures of human NEET proteins

Three crystal structures of the soluble region of mNT were reported and in principal they were essentially identical [24–26]. Our group obtained the crystals at neutral pH conditions under which mNT was more stable. Multiwavelength anomalous diffraction (MAD) was utilized to obtain model-independent phasing information for the three-dimensional structure [24]. Concurrently, another group obtained and presented the structure of mitoNEET [25], and shortly after the third structure was published [26]. Surprisingly, the structure showed no

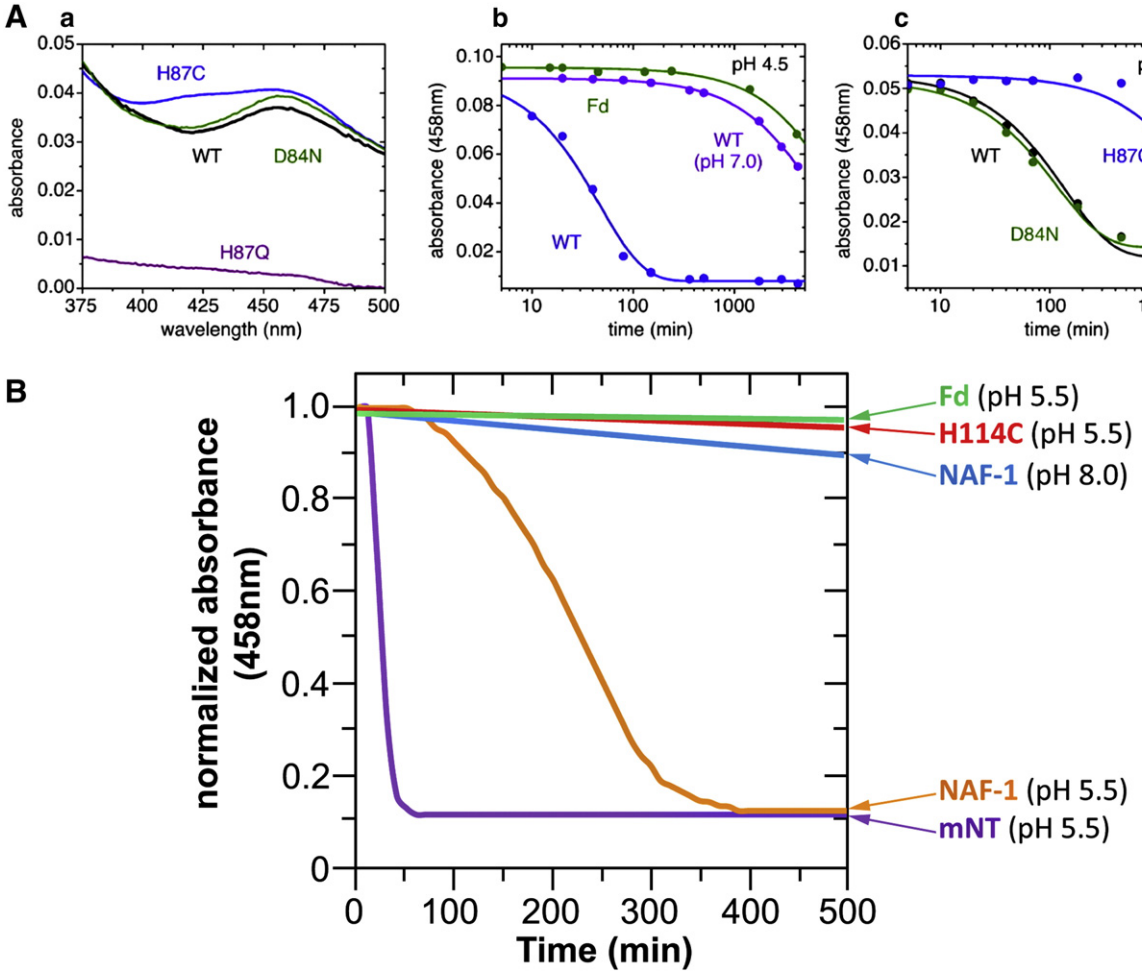

Fig. 2. The 2Fe–2S cluster of NEET proteins is pH-labile. (A) *MitoNEET cluster stability*; the absorbance and stability of the Fe–S cluster of mitoNEET were monitored at 458 nm in wild type (WT) and mutant mNT proteins as a function of time at different pH. (a) Optical spectra of WT (black), D84N (green), H87C (blue), and H87Q (violet) mitoNEET proteins. (b) Stability of the 2Fe–2S cluster of mitoNEET at pH 7.0 (purple) and 4.5 (blue) when compared with that of ferredoxin (Fd), monitored at 420 nm at pH 4.5 (green). (c) Stability of the 2Fe–2S cluster of WT (black), D84N (green), and H87C (blue) mitoNEET at pH 6.0 as a function of time. Note that the H87C mutation affects the visible spectrum and the stability of the Fe–S cluster of the mutant mitoNEET [20]. (B) *Destabilization of NAF-1 2Fe–2S cluster*: Similar to mNT, the stability of the NAF-1 2Fe–2S cluster is dependent on pH, at pH 8.0 NAF-1's cluster is more stable than at pH 5.5 (blue and orange, respectively). At pH 5.5, NAF-1's cluster is more stable than mNT's cluster (orange and purple, respectively). The stability of NAF-1 was compared with that of Fd and NAF-1 mutant H114C (green and red, respectively) [23]. Buffers used in A and B are different.

similarity to any of the, at-the-time, 45,000 deposited structures, of which 650 were 2Fe–2S proteins (Fig. 3). Unexpectedly, the protein was a homodimer, and contained a unique fold termed the "NEET fold" [24]. The structure clearly indicated two distinct domains; a beta-cap and a 2Fe–2S cluster binding domain (Fig. 3A). The cluster binding domain is in general more hydrophilic and charged, whereas the beta cap domain contained a hydrophobic core (Fig. 3B, C).

Sequence alignment and early mutagenesis experiments [20] identified the potential ligands of the mNT 2Fe–2S cluster assuming that it was monomeric, an assumption that was proved wrong by the crystal structures. The structures provided unambiguous details of the Fe–S binding region, indicating that the outer Fe atom is coordinated by one Cys and one His side chain. This unique coordination of the Fe is a type of hybrid between the ferredoxin proteins that bind the outer Fe with two Cys and the Rieske proteins that bind the outer Fe with two His [27] (Fig. 4).

The N-terminus of the NEET constructs, composed of amino acid side chains that connect the transmembrane helix to the cytoplasmic C-terminal cluster binding domains, is generally not resolved in the crystal structures. In some cases, in which the N-termini were resolved, the N-termini of the two protomers showed different conformations resulting from different interactions with the N-termini of symmetry related molecules [28]. These results indicate that there is flexibility leading to multiple conformations of the N-termini in the soluble constructs that can be trapped in different orientations within a crystal. For example, the structure presented in RCSB PDB ID: 2R13 [26] showed completely different orientations and secondary structure of the N-termini than those in RCSB PDB ID: 3EW0 [28]. Thus, the N-termini of the soluble crystallized NEET constructs, which reflect the amino acids linking the transmembrane helix to the ordered cluster binding domains in the full length protein, are not well structured providing evidence that the linker region is flexible (Fig. 5). This may be important for interactions with the OMM, with other membrane-bound proteins and/or with soluble cytosolic proteins.

Crystals of the soluble region of the human paralog NAF-1 (Miner1) were obtained under similar conditions to mNT [21]. The crystal structure was solved to a resolution of 2.1 Å (R-factor = 17%). As with mNT, NAF-1 is a homodimer harboring two redox-active 2Fe–2S clusters, one on each protomer (Fig. 3). As NAF-1 was shown to be causative in Wolfram Syndrome 2 [14], the NAF-1 structure showed for the first time an association of a redox-active Fe–S protein with this disease (see more details below). As in mNT, each 2Fe–2S cluster in NAF-1 is bound by the same rare 3Cys–1His motif within a 16 amino acid segment. However, it should be noted that there is a change in the beta

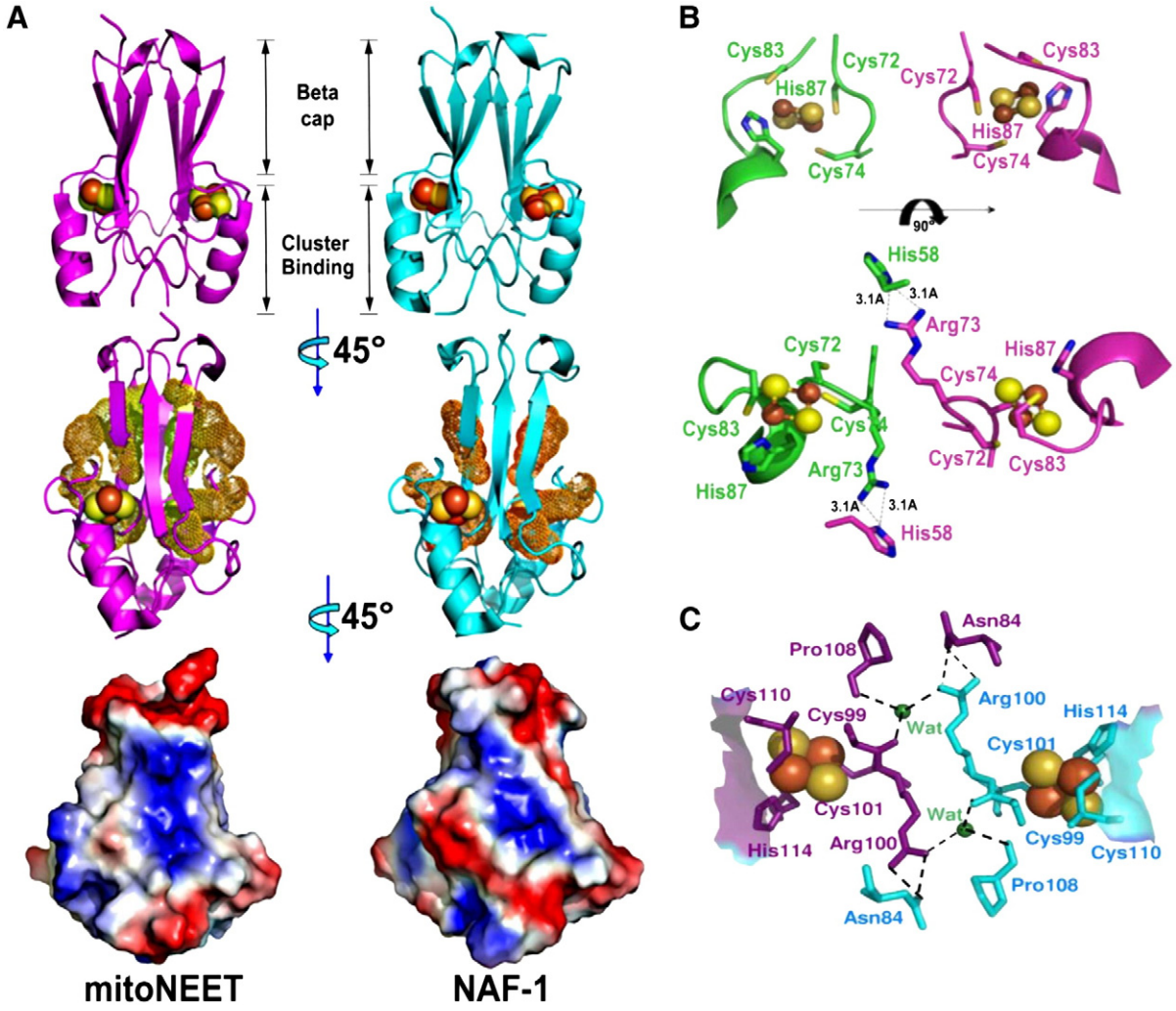

Fig. 3. Structural comparison of the human NEET proteins mitoNEET (PDB ID: 2QH7) and NAF-1 (PDB ID: 3FNV). (A) (a) The overall structure of both proteins is homodimeric, has a very similar backbone fold and harbors two 2Fe–2S clusters in the same juxtaposition. (b) There are notable differences in the hydrophobicity between NAF-1 and mNT as shown by the differences in the distribution of aromatic side chains shown in yellow. (c) There are notable differences in the surface shape and charge distributions (red — negative, blue — positive) of the two proteins. (B) Details of the 2Fe–2S cluster binding site of mitoNEET highlighting the coordinating ligands and a nearby interprotomer interaction. (C) Details of the NAF-1 cluster binding regions. NAF-1 shares the same coordination as found in mitoNEET and also the similar key interprotomer interactions with His58 of mitoNEET being Asn84 of NAF-1.

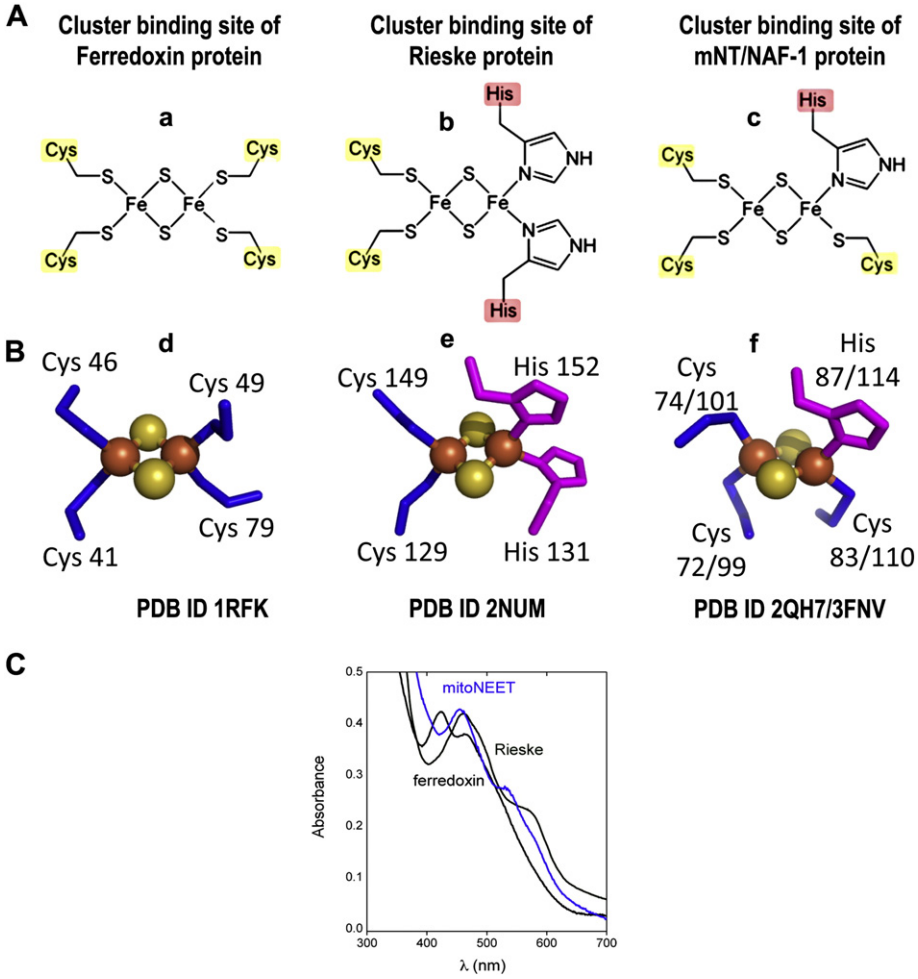

Fig. 4. Comparison of the 2Fe–2S cluster of ferredoxin (PDB ID: 1RFK), Reiske (PDB ID: 2NUM) and human NEET proteins (mNT PDB ID: 2QH7 and NAF-1 PDB ID: 3FNV). (A–B) *Structural comparison of the 2Fe–2S coordination*. Structures of NEET proteins (c, f) reveal the details of the Fe binding to the proteins. They indicate that the outer Fe (the right-most iron atom) is bound by one Cys and one His. This unique coordination of the Fe being a type of hybrid between the ferredoxin proteins (a, d) that bind the outer Fe with two Cys and the Rieske proteins (b, e) that bind the outer Fe with two His. (C) *The absorption peaks of the 2Fe–2S clusters in the different proteins*. UV–vis spectra were distinct (ferredoxin, black; mitoNEET, blue; Rieske, green). The mitoNEET 2Fe–2S cluster absorbance peak is more similar to that of the Rieske 2Fe–2S cluster that is coordinated by 2Cys:2His.

cap domain that contributes to changes in the stability properties of the 2Fe–2S clusters of NAF-1 [21]. Importantly, there are also significant differences in the surface charge and hydrophobicity that contribute to the specificity in possible interactions by NAF-1 with protein partners, *vs.* its analogue mNT (Fig. 3A–C).

As the single His ligand is a hallmark of NEET proteins (Fig. 3B & C) and replacement of the single His ligand with Cys (in mNT H87C mutant) results in large changes to the properties of mNT ([20], and see below), we determined the structure of the H87C mutant under similar conditions used to determine the native structure [28]. All structural changes in the H87C mutant were found to be localized to the region near the site of the mutation. The Cys87 was found to be in two conformations as well as the Lys55 which forms hydrogen bonds with the native His87. No other changes were observed in the crystal structure indicating that changes to the 2Fe–2S cluster properties resulted from localized effects. More recently, we also determined the structure of the equivalent mutation in NAF-1, H114C (29). In this case, a single conformation of Cys was determined. As with mNT, in the H114C NAF-1 mutant a change in the nearby Lys (Lys81) was identified. The high structural similarity (almost identical) between the native NAF-1 and H114C mutant shows that the biophysical, biochemical and biological differences between these two variants are primarily due to the change in the 2Fe–2S ligation of these proteins.

2.3.2. Structures of other orthologs of NEET proteins

The NEET family of proteins is ancient being found in all domains of life [30]. The human NEET ortholog from the plant *Arabidopsis thaliana* was recently found to have the same NEET fold and cluster ligation (Fig. 6A) as the human mNT/NAF-1 proteins, but differed in its surface electrostatics and hydrophobic properties [31].

Bacteria were found to have NEET orthologs that are more similar to Miner2, being a single polypeptide harboring two 2Fe–2S clusters (Fig. 6B). The fact that the 3Cys:1His coordinated 2Fe–2S clusters are conserved from bacteria to humans suggests an important ancient role for these proteins in basic cell survival functions. Using bioinformatics tools such as domain fusion and phylogenetic analysis, many of the bacterial NEET homologs were found fused to redox active proteins [30]; a finding that supports an ancient role for NEET proteins in electron transfer reactions. One of the non-fused prokaryotic versions, isolated from *Magnetospirillum magneticum* AMB-1, an aquatic alpha bacterium that utilizes iron reduction to derive energy, was presented as a bacterial ortholog of Miner2 [30]. The structure of this protein revealed an overall fold that is quite similar to that of mNT and NAF-1 with two 2Fe–2S clusters, each coordinated by the hallmark 3Cys:1His (Fig. 6B). The major difference was that as opposed to mNT and NAF-1, the Miner2 ortholog, is a monomer, not a homodimer (Figs. 3 & 6B), and its two 2Fe–2S clusters are bound at two different parts of the sequence of the single

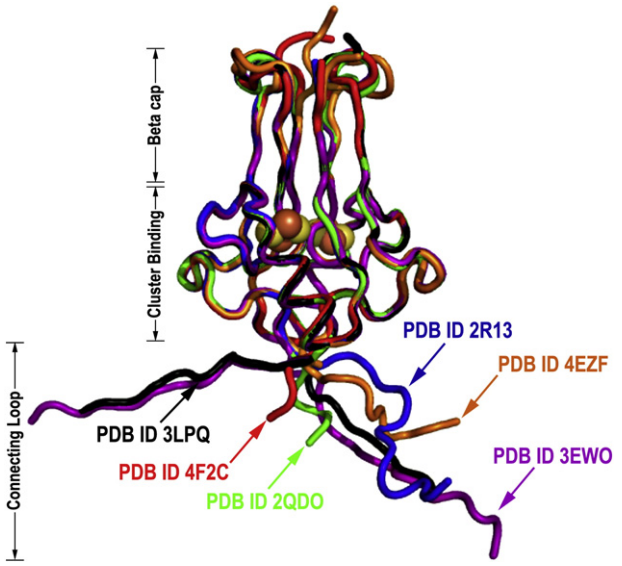

Fig. 5. The connecting soluble-membrane region of the NEET proteins shows high degree of flexibility. NEET proteins are composed of two stable structural domains that comprise most of the soluble region of the proteins, the beta-cap and cluster-binding domains. The N-terminal region includes a transmembrane helix and a segment that connects the soluble domains to the helix. This connecting loop shows a high degree of flexibility. The latter is clearly evident when various structures of the mNT proteins are superimposed.

polypeptide. All of the NEET orthologous structures appear therefore to share several common features: the presence of a cluster binding domain and a beta cap domain and the presence of two 2Fe–2S clusters each bound by 3Cys and 1His in essentially the same relative juxtaposition with respect to each other with internal (pseudo) dyad symmetry.

2.4. Biophysical properties of the NEET 2Fe–2S clusters

The unique 3Cys:1His coordination of NEET proteins enabled the comparison of their biophysical properties to that of ferredoxin and Rieske proteins that have the outer Fe of their 2Fe–2S cluster coordinated with two Cys or two His, respectively (Fig. 4, above). The three general techniques utilized for such comparison were EPR (*E*lectron *P*aramagnetic *R*esonance) which senses the environment of the unpaired electrons in transition metal centers in proteins, resonance Raman spectroscopy which monitors vibrational transitions coupled to an electronic transition of the oxidized 2Fe–2S cluster, and redox (reduction/oxidation) potential measurements which is a measure of the ease of transition from the oxidized to the reduced state (Fig. 7). The results obtained from each of these biophysical methodologies are described below.

To investigate the electronic structure of the NEET cluster in its reduced state, we used multi-frequency and multi-technique EPR spectroscopy [32]. The reduced cluster was found to have a rhombic *g* tensor with an average *g* value of 1.947 that falls between those of Rieske-type and ferredoxin-type $[2Fe–2S]^{2+}$ clusters (Fig. 7A). From simulation and least-squares fitting of the multitude of data, we inferred the absolute *g* tensor orientation with respect to the cluster. Importantly, in X-band (9 GHz microwave frequency) ENDOR (*E*lectron *N*uclear *DO*uble *R*esonance) and ESEEM (*E*lectron *S*pin *E*cho *E*nvelope *M*odulation) spectra, a coupled nitrogen is visible, attributed to the Nε of the histidine in the protonated state. The latter is absent in the H87C mNT mutant, in which the cluster is coordinated by 4 Cys. We found that the native cluster is in a valence-localized state, where the electron is localized to the outer iron bound by the His. The field-sweep spectra showed evidence of inter-cluster dipolar coupling, indicating that the clusters interact with each other (Fig. 7A). Similar results were reported for the rat homolog of mNT [33]. These parameters can be considered as reporters of the NEET proteins in general, and of how their cluster structure is altered upon a change in its environment. The coupling observed between the clusters show that they communicate and could undergo intra-dimer electron transfer. Furthermore, the coupling implies that changes to one 2Fe–2S cluster can affect the properties of the other 2Fe–2S clusters.

Interestingly, the EPR results are comparable to previously published data from 1978 on Fe–S proteins in mitochondria. Isolation of the OMM yielded an X-band EPR spectrum showing the presence of two types of 2Fe–2S clusters [34,35]. The spectra they observed are essentially identical to that found for the homodimeric mNT; the two apparent types of clusters due to spectral splitting caused by the interaction between the clusters within the homodimer. Importantly, this shows that the proteins harbor redox active 2Fe–2S cluster *in vivo*.

To study the oxidized state of the 2Fe–2S cluster, resonance Raman spectra was used to characterize this naturally occurring 3Cys:1His 2Fe–2S protein and to assess local structural changes associated with its cluster lability (Fig. 7B) [36]. Comparison of mNT to its ferredoxin-like mNT H87C mutant, in which the cluster is coordinated by 4-Cys,

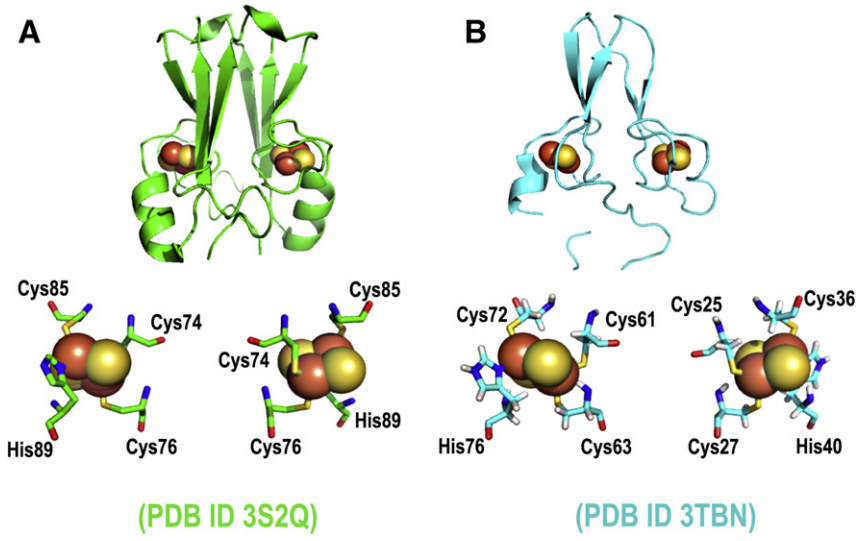

Fig. 6. Structure of NEET homologs from other organisms. (A) Structure of the NEET protein from *Arabidopsis* (PDB ID: 3S2Q). It is homodimeric as are the human mitoNEET and NAF-1. (B) Structure of the Miner2 ortholog from *Magnetospirillum magneticum* AMB-1 (PDB ID: 3TBN) [30]. In this case, a single polypeptide binds two 2Fe–2S clusters in a very similar juxtaposition as found in the homodimeric NEET proteins.

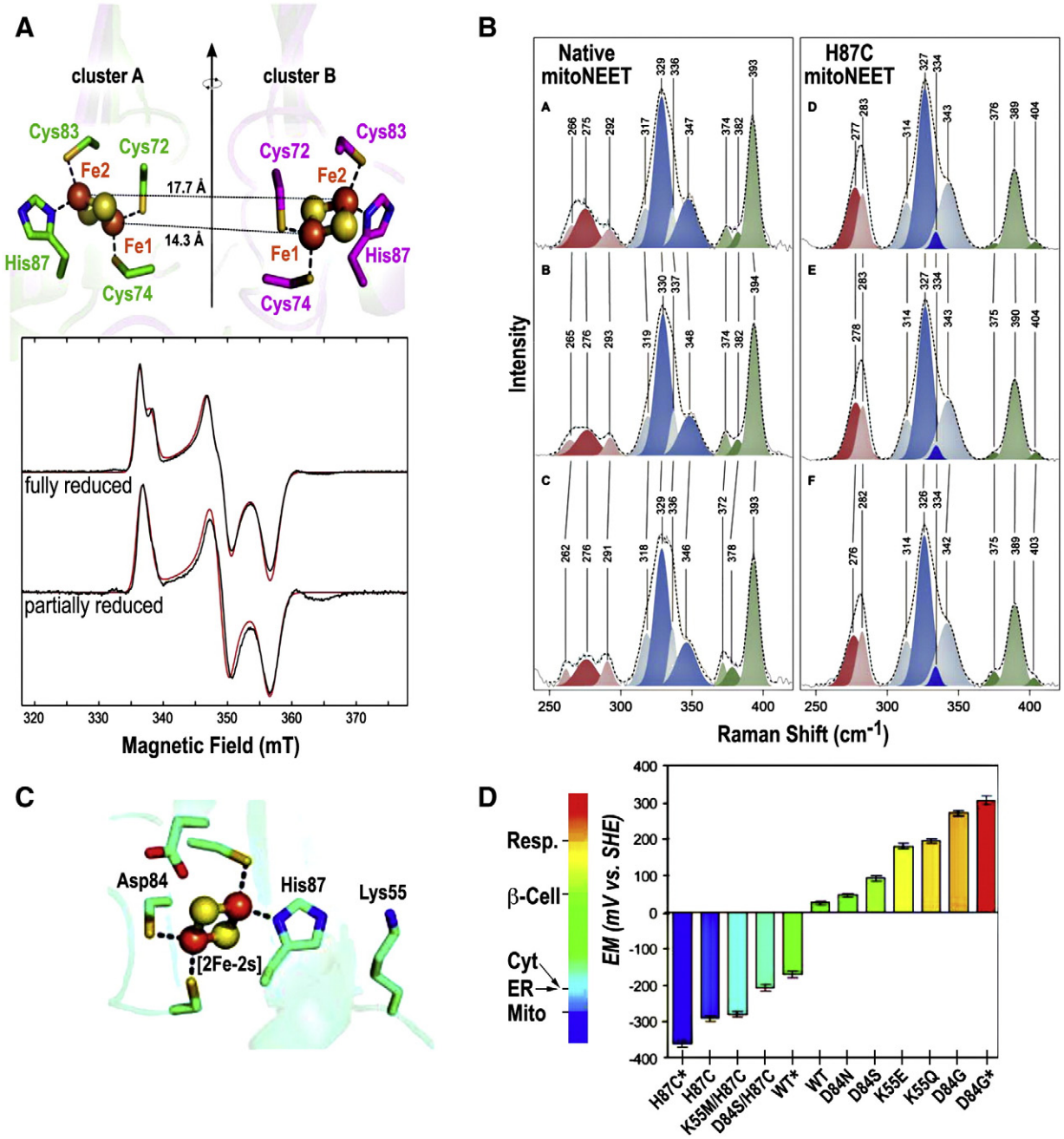

Fig. 7. Electron paramagnetic resonance, resonance Raman and redox characterization of mitoNEET. (A) Relative orientation of the two 2Fe–2S clusters of homodimeric mitoNEET based on the structure (PDB ID: 2QH7). EPR spectra of the fully reduced and partially reduced mitoNEET are shown below. Note that the splitting in the low field region (near 335 mT) is absent in the partially reduced sample reflecting the absence of the intercluster interaction [32]. (B) Resonance Raman spectra of oxidized native (A–C) and H87C (D–F) human mitoNEET as a function of pH; pH decreases from top to bottom. Note the differences in the low frequency region (250–300 cm^{-1}) between native and H87C showing that this region is sensitive to the His87. Also note that this region shows pH sensitivity in the native but not the H87C mutant mitoNEET [36]. (C, D) Redox range of mutant mitoNEET proteins. (C) Part of the structure near the 2Fe–2S clusters highlighting residues important for modulating the redox potential. (D) Measured redox potentials of mutants that both decrease and increase the redox potential by >300 mV giving a total unprecedented range of approximately 700 mV. Typical cellular redox potentials are shown on the bar next to the plot. Mutant redox potentials span the entire range [47].

indicated that Raman peaks in the approximately 250–300 cm^{-1} region of mNT are influenced by the Fe–His87 moiety. Systematic pH-dependent resonance Raman spectral changes were observed in this spectral region for native mNT but not the H87C mutant. The approximately 250–300 cm^{-1} region of native mitoNEET is also sensitive to phosphate buffer, which stabilizes the cluster from release [36] and was shown to bind near His87 in the crystal structure [37]. Thus, conditions that influence cluster release were shown to be concomitantly affected by the resonance Raman spectrum in the region with Fe–His contribution. These results support the hypothesis that the Fe–N(His87) interaction is modulated within the physiological pH range, and this modulation may be critical to the function of mNT.

To determine the energy required to reduce the 2Fe–2S cluster we used both protein film voltammetry (PFV) and optical potentiometric measurements to investigate the redox potential under different conditions and in native and mutant proteins. Using either method, the redox potential of mitoNEET was near 0 mV at pH 7.0. Because addition of higher concentrations of TZDs to buffered solutions results in insoluble precipitate that interfered with optical methods, PFV was employed as a mean to demonstrate the direct impact of TZD drug binding on the

redox chemistry of the Fe–S cluster. When TZDs bind, the midpoint potential at pH 7 was lowered by more than 100 mV, shifting from approximately 0 to −100 mV. This shift shows that the TZD prefers to bind to the oxidized state [38]. In the H87C mutant the redox potential was decreased nearly 300 mV due to replacing the His ligand with a Cys. This moved the redox potential in the range more common to ferredoxin-like proteins with 2Fe–2S clusters coordinated with 4-Cys (recently reviewed for iron–sulfur proteins in Bak and Elliott [39]). Importantly, the addition of TZDs had no effect on the redox potential in the H87C mutant, showing that the drug binding is weaker in the mutant and suggesting that the drug interacts near His87 [38].

Redox potential measurements can also be used for titration of key amino acid residues by measuring the variation in the redox potential as a function of pH. Although these measurements provide a wealth of information, the interpretation is model-dependent. As previous results indicated the importance of His87 for stability and spectroscopic properties, we wanted to determine the pKa values for the key His87 ligand; there are two pKa values, one associated with the oxidized state and one associated with the reduced state of the 2Fe–2S cluster. Two different methods were utilized — one was measurement of the redox potential of protein in solution using optical potentiometric methods and the other using protein bound to a surface using protein film voltammetry. The values and pH profiles of the two methods were in general agreement [38,40,41]. The pH dependence of mNT displayed nearly classic behavior in the decrease of E_m *versus* pH for a single titrating site. However, for quantitative fit to the data, a second term needed to be included. One model included a second titrating site which provided an improved fit and could be applied to a comprehensive set of mutants investigating the hydrogen bonding interactions near the 2Fe–2S clusters [40]. An alternative model included an empirical term to account for deviations from an ideal slope; this term was to account for the net effect of numerous small effects that occur over the pH range of the measurements without specific assignments of pKa values. This latter model was applied to a set of mutants designed to extend the range of redox potentials through amino acids in the vicinity of the 2Fe–2S clusters to exact mainly the pKa values for His87 [41]. Both models provided a similar value for the pKa of His87 in the oxidized state of ~7. However, they made quite different predictions in the pKa of His87 in the reduced state. To distinguish between the models, we employed a more direct method using optical titration of the 2Fe–2S cluster absorption bands. The basic idea is that as His87 protonates, the interaction between His87 and the 2Fe–2S cluster is perturbed resulting in a change in the energy of electronic transition (ligand to metal charge transfer bands) and, hence, a change in the optical spectrum. This allowed us to directly titrate the ligands to the 2Fe–2S cluster and the results showed unambiguously that the pKa of His87 in mNT is 6.8 (oxidized) and 12.4 (reduced) favoring the latter model as a better description of the His87 interactions. Although this model provides better values for the interaction, it introduces an empirical parameter that cannot be directly related to amino acid titrations. Thus, neither model on its own provides a complete satisfactory description of the observed behavior warranting further more sophisticated refinements to the modeling. Nevertheless, the large change in the pKa values (~5.6 units) of His87 reflects a very strong interaction between it and the 2Fe–2S cluster consistent with the EPR and resonance Raman studies discussed above.

Next we tested the ability to vary the redox potential of the clusters. The ability to "tune" an 2Fe–2S cluster redox potential over a wide range had been limited in many other 2Fe–2S proteins by instability of the clusters upon mutation of amino acids at or near the clusters [41]. Nevertheless, we were able to mutate key residues near the 2Fe–2S cluster and obtain, for most mutations, proteins with intact and redox-active clusters. From the set of mutations stable enough to obtain good redox measurements, we were able to vary the redox potential over an unprecedented range of ~700 mV and with the ability to both increase and/or decrease the redox potential to span the entire range of potentials reported in cellular environments (Fig. 7C) [41]. Some additional mutations were also recently reported to fall within this range [41]. Overall, mNT is quite tolerant to amino acid substitution at and near the 2Fe–2S cluster binding sites, making it a great model system for studying the "tuning" of redox potentials. The redox potentials of NAF-1 were also measured and found to be essentially the same as that of mNT [21,29]. The redox potential of NAF-1 similarly displayed a strong dependence on pH above pH 7 showing that electron reduction is also coupled to protonation. In both mNT and NAF-1, we recently discovered that long-range allostery can also tune the 2Fe–2S potential.

2.4.1. Allostery in mNT affects its 2Fe–2S cluster properties

Recently, the importance of allostery in mNT was explored both theoretically and experimentally (Fig. 8) [42]. It was found that a loop (L2) 20 Å away from the 2Fe–2S cluster exerts allosteric control over the cluster's redox properties. Substitution of amino acid side chains of L2 resulted in shifts of up to 100 mV in the redox potential of the 2Fe–2S clusters and a more than 15-fold change in the rate of 2Fe–2S cluster transfer to an apo-acceptor protein (see below). These surprising effects occur in the absence of any crystallographic structural changes. An examination of the native basin dynamics of the protein using all-atom simulations shows that twisting in L2 controls scissoring of the cluster binding domain that results in perturbations to one of the cluster-coordinating histidines. These allosteric effects are in agreement with previous folding simulations that predicted L2 could communicate with residues surrounding the metal center [43]. They resemble similar allosteric cross-talk reported for the ferredoxin 4-Cys coordinated protein [44]. Our findings suggest that long-range dynamical changes in the protein backbone can have a significant effect on the functional properties of NEET proteins and suggest possible allosteric regulation of the cluster properties and function.

Taken together, the mNT/NAF-1 biophysical characterization by numerous methodologies supports two possible cellular functions for NEET proteins (Fig. 9): i. cluster transfer function (Fig. 9, blue arrows) and/or ii. electron transfer function (Fig. 9, purple arrows).

3. Cellular and whole organism function of NEET proteins

In recent years, building upon the detailed biophysical characterization of NEET proteins, some of the research of NEET proteins shifted towards understanding their biological/cellular/whole organism function(s). In parallel, the involvement of mNT and NAF-1 in different pathologies, as well as in health (longevity) has emerged as highly important.

3.1. NEET proteins as cluster donor proteins

One of the possible cellular functions of NEET proteins initially suggested for mNT based on the earlier biophysical results was *cluster transfer* (Fig. 9). Because the His87 of mNT and the His114 of NAF-1 can undergo changes in protonation near neutral pH, protonation was suggested to be a "gate" or "trigger" for cluster release/transfer [24]. A similar coordination (with a histidine present) was proposed for human IscU (*I*ron *S*ulfur *C*luster assembly enzyme *U*) based on the crystal structure of a bacterial homolog [45]. This similarity in the coordination of the 2Fe–2S cluster, in addition to the fact that the 2Fe–2S cluster appears to be labile by design, strengthens the hypothesis that NEET proteins may be able to perform a similar biological function as *cluster donor proteins* that transfer their 2Fe–2S cluster to *an apo-acceptor protein*. For this transfer to occur, and to have an experimental system to test it, an appropriate apo-acceptor had to be found. To date the physiological apo-acceptor protein(s) of NEET proteins was not identified, and since the apo-acceptor gold standard of such studies [46] is apoferredoxin (apo-Fd) this protein was tested as a possible cluster acceptor protein. The fact that the ferredoxin (Fd) cluster is tightly coordinated by the 4-Cys coordination (see Fig. 4, above), secures a tighter binding of the cluster to Fd following the cluster transfer and facilitates a *uni-*

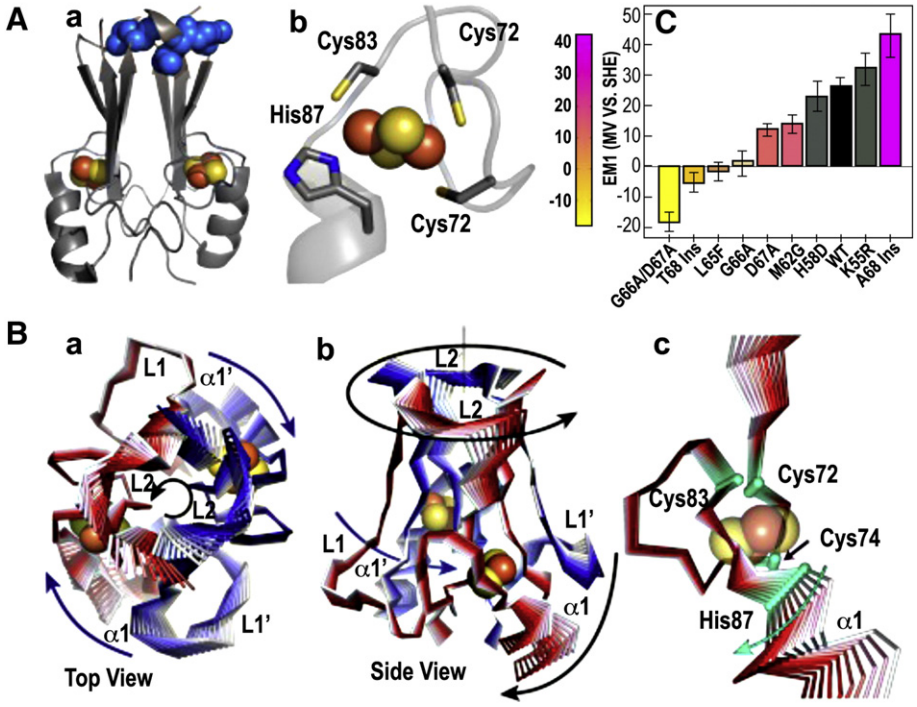

Fig. 8. Effect of allostery in mitoNEET function. (A) Replacement of distal residues in a loop at the top (L2) result in both positive and negative shifts in the 2Fe–2S cluster redox potential at pH 7 ($E_{M,7}$). (a) Mutated residues in L2 are colored in blue on the structure of mitoNEET. (b) Coordination of the [2Fe–2S] remains unaltered in the mutant mitoNEET crystal structures. (c) $E_{M,7}$ values for WT mitoNEET and L2 mutants span a range of ~60 mV (SHE values). (B) Twisting in L2 controls swinging of His87. (a) Ten frames from the collective motions of the Cα atoms for the first eigenvector are superimposed on the structure. The initial starting point is colored white, with each subsequent frame moving from white to red for protomer A and white to blue for protomer B. From the top view, the protein exhibits a torsional motion with the loops twisting together at the top of the beta-cap domain in the foreground, and the cluster binding domain moving in the opposite direction in the background. (b) The side view of the protein shows that the twisting of the β-cap domain results in scissoring of α1 and L1′ with α1′ and L1 in the cluster binding domain, with the [2Fe–2S] cluster acting as a hinge point. (c) The backbone of the cluster-coordinating pocket and the coordinating cysteines shows little movement; however, the coordinating histidine swings open in response to twisting in L2. These computational results provide a framework to interpret the experimental finding that properties of the cluster can be altered by distant mutations without changes to the crystal structure [42].

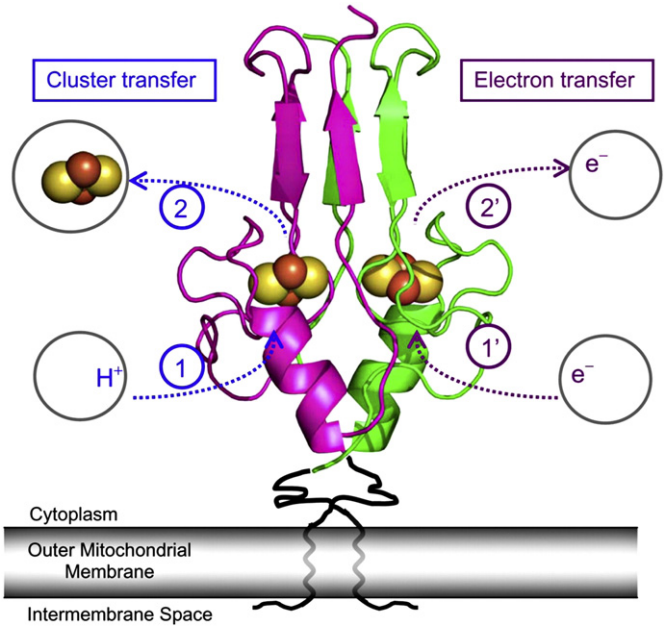

Fig. 9. Proposed functional roles of the NEET proteins. MitoNEET is shown linked (magenta and green) to the OMM (gray) (not to scale). On the basis of mitoNEET biophysical properties, two possible functions are suggested: cluster transfer (blue arrows) and electron transfer (purple arrows). The left side shows possible cluster transfer reactions. The right side (purple) shows possible reduction reactions of the 2Fe–2S clusters. Biophysical and biochemical results show that His-87 is a key ligand for cluster transfer (release) and tuning the redox potential [24].

directional transfer from the NEET protein. As shown in Fig. 4C, the donor and acceptor proteins can be distinguished spectroscopically — the Vis spectra of NEET proteins has a peak absorption at 458 nm which is distinct from that of Fd which has a peak absorption at 423 nm. The latter results from the difference in the coordination of the 2Fe–2S clusters and is reflected in the Vis spectra as ligand-to-charge transfer bands. Another prerequisite for a cluster transfer process to occur is that the NEET protein and Fd should have the ability to bind one another. Fig. 10 shows that NAF-1 and Fd association is possible (Fig. 10A, B) and that a cross-linker (Fig. 10C) can even enforce a permanent association (Fig. 10D, E). Fig. 11 shows that cluster transfer can occur when NAF-1 is incubated with pre-reduced apo-Fd in which the sulfur atoms of the cysteines in the cluster binding site are reduced (free thiol-SH) [29,47]. The reduction of the cysteines in the cluster binding site of the acceptor protein was successfully performed both by chemical reducing agents such as β-mercaptoethanol or sodium dithionite dithiothreitol (DTT), and by natural, biological reducing agents found in living cells such as glutathione or thioredoxin [23,47]. Cluster transfer studies indicated that in order for the transfer to occur, the cluster of the donor protein has to be in its oxidized $[2Fe–2S]^{2+}$ state.

In the NEET cluster transfer assays (Fig. 11), incubation of holo-NEET and pre-reduced apo-Fd *in vitro* indicated, both by native gel and optical spectroscopy, that NEET proteins transferred their iron–sulfur cluster to apo-Fd forming holo-Fd with a concomitant decrease in holo-NAF-1. The two methods provided complementary confirmation of the transfer. The difference in visible spectra of the NEET donor and Fd acceptor provided us with a spectroscopic fingerprint of the process as transfer takes place (Fig. 11C). The difference in their migration rates in native-gels provided a more visual picture of the transfer process (Fig. 11B). The

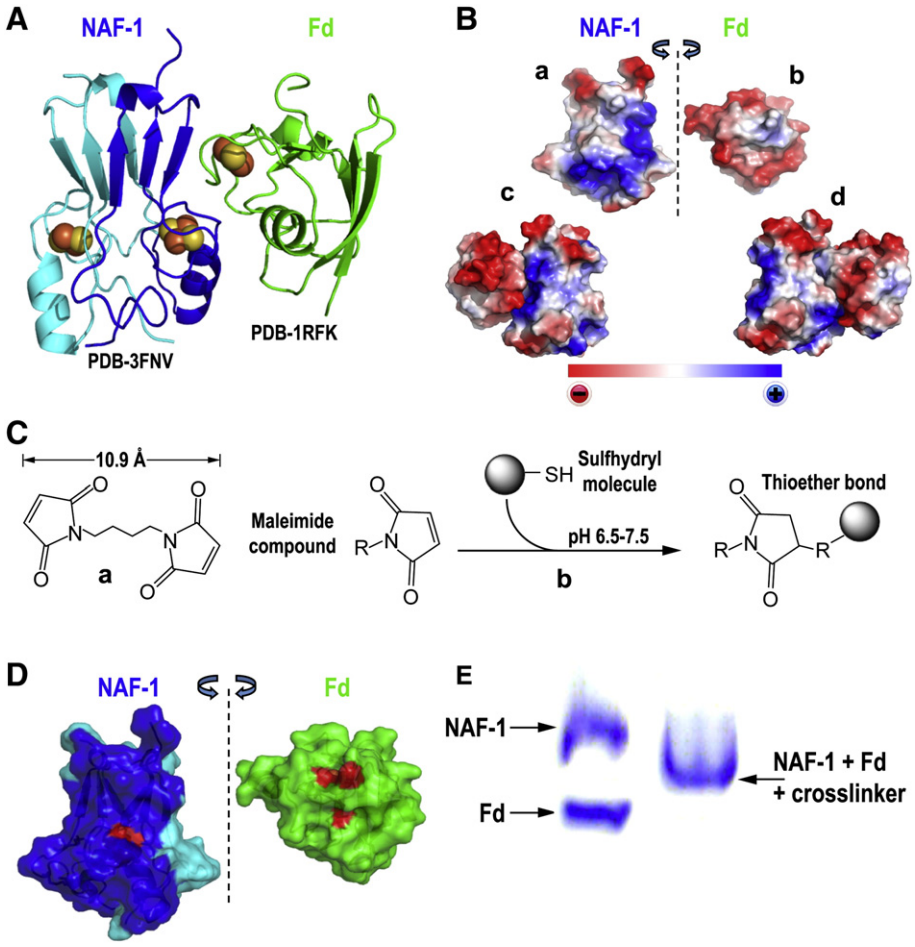

Fig. 10. The NEET protein NAF-1 and apo-Fd can interact as cluster donor and cluster acceptor proteins, respectively. (A) A protein–protein complex model of NAF-1 (blue) and Fd (green) suggested after a global docking run by the ClusPro docking server [117]. The obtained lowest energy models place the clusters side-by-side with few different orientations. (B) The calculated surface charge maps of NAF-1 (a) and ferredoxin (b) show the blue-cationic and red-anionic residues demonstrating the structural complementarity. (a) and (b) panels show the surface of each protein at the area of binding and (c) and (d) panels show the interacting proteins. (C) BMB crosslinker's molecular scheme (a) and reaction of maleimide-activated compounds to sulfhydryls (b). (D) Surface of NAF-1 (blue) and Fd (green) at the area of binding. The cysteine residues from the cluster binding domains are colored red. (E) The mixture of NAF-1 and (apo) Fd together with the crosslinkers BMB results in a new pattern of bands (right-hand lane) on a native gel compared to the lane that consists the proteins without the cross-linker (left-hand lane).

uni-directional cluster transfer from a NEET protein to apo-Fd is schematically demonstrated in Fig. 11A.

By monitoring the spectra as a function of time, we were able to show that mNT could transfer its 2Fe–2S cluster to a canonical ferredoxin acceptor (Fd) with an almost 100% transfer efficiency and, surprisingly, at a rate comparable to cluster transfer rates reported for an iron–sulfur assembly protein (Fig. 12). These results underlined the hypothesis that at least one function of NEET proteins in cells is 2Fe–2S cluster transfer (Fig. 12). To investigate the importance of His87 in the cluster transfer function, we measured the extent and rate of transfer from the H87C to Fd. The mutant showed essentially no cluster transfer over the time of the experiment (half time >30× that of native mitoNEET). Thus, His87 is particularly important for the cluster transfer process.

The ability to measure cluster transfer provided a second functional assay, on top of cluster stability assays [47], for measuring small molecule binding and for investigations of protein–protein interactions. In addition, determination of the rates of cluster transfer provided a measure of the protein dynamics upon mutation as changes in regions calculated to be very dynamic parts of the structure resulted in changes of up to 15-fold in the rate of transfer of the 2Fe–2S clusters to Fd [42].

The ability of NAF-1 to function as a cluster donor was also tested and found to be similar to that of mNT [23]. Although the ability of Miner2 to transfer its clusters has not been established, the similarities between this protein and mNT or NAF-1 suggest that a similar cluster transfer function could also be assigned to this protein. Moreover, since the ability to transfer the 2Fe–2S cluster in its entirety and without loss has only been observed in proteins involved in cluster assembly or transfer, our findings that mNT and NAF-1 satisfy those conditions suggest their potential involvement in cluster assembly/transfer processes.

3.2. NEET proteins' cluster/iron transfer to mitochondria in cells

The NEET proteins unique cellular localization (on the cytosol-facing membranes of the ER and mitochondria), enable in principle, their function as cluster/iron transfer protein into- and out of these organelles. In order to test whether the transfer of cluster/iron into the mitochondria is at all possible, and to characterize the ability of NEET proteins to transfer their cluster/iron *in situ*, in cells, *R*hodamine B-[(1,10-*P*henanthrolin-5-yl)-*A*minocarbonyl]benzyl ester (RPA), a fluorescent metal sensor that accumulates within mitochondria of living cells, was used. RPA is the conjugate of the cationic fluorophore rhodamine and the iron chelator phenanthroline. When iron binds to the chelator phenanthroline, the fluorescence of RPA is quenched (Fig. 13A). RPA fluorescence could therefore be used as a reporter of iron levels within mitochondria [48–50]. To test for the ability of NEET proteins to transfer their Fe/Fe–S

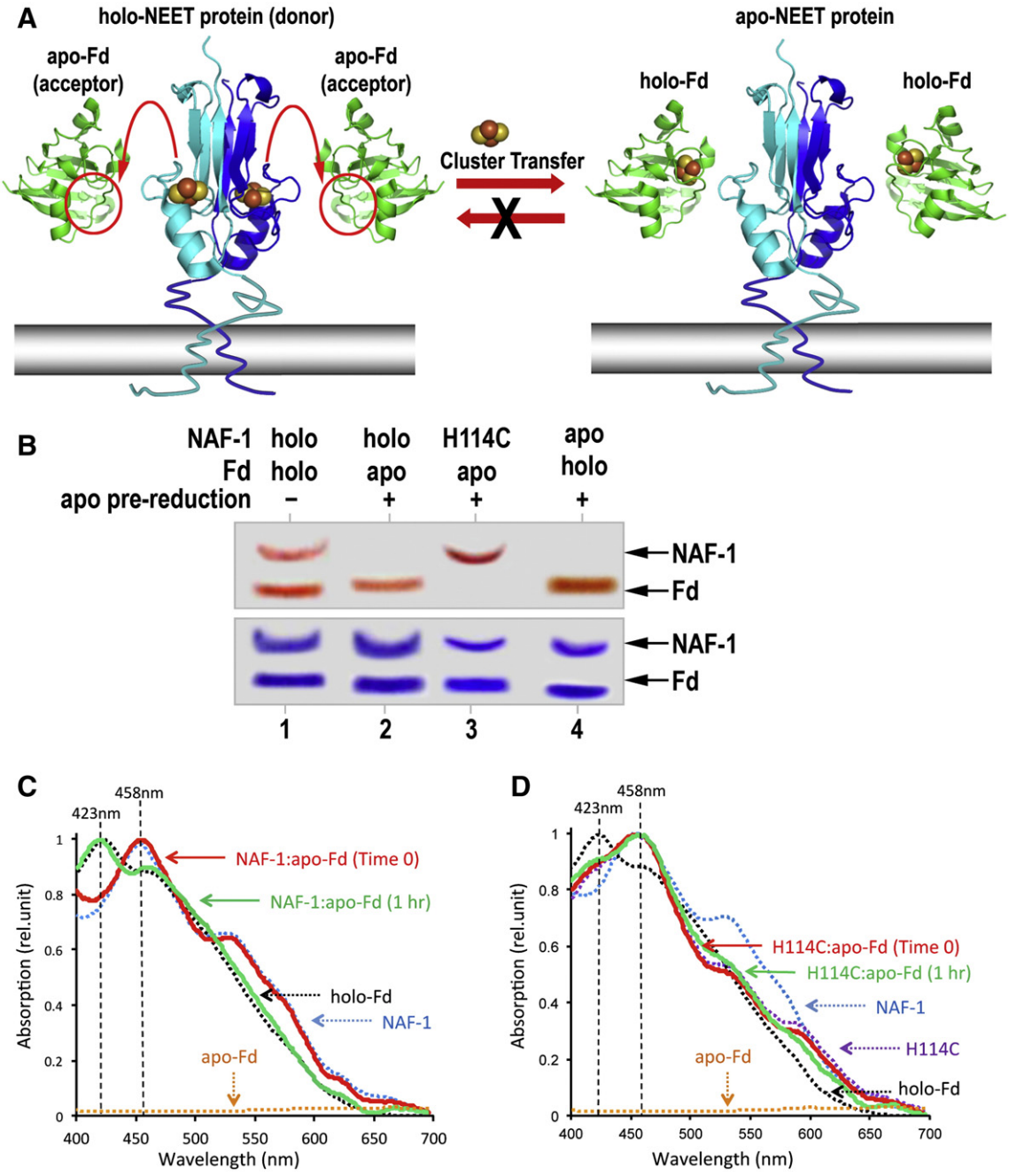

Fig. 11. Optical spectroscopy and Native-PAGE are among the analytical methods to follow cluster transfer from NEET protein (donor) to apo-Fd (acceptor) to obtain holo-Fd. (A) A schematic representation of cluster transfer from NAF-1 to apo-Fd. (B) NAF-1 was incubated at 37 °C with a β-mercaptoethanol-reduced apo-Fd for 30 min and the products were run on a native gel. The Native-PAGE following the cluster transfer from holo-NAF-1 to apo-Fd (lane 2), holo-NAF-1 mutant H114C to apo-Fd (lane 3) and holo-Fd to apo-NAF-1 (lane 4). Holo-NAF-1 and holo-Fd are shown for reference (lane 1). The red colored bands are indicative of the [2Fe–2S] cluster in the two proteins; the upper red band represents NAF-1 (labeled NAF-1 on the right side of the gel) and the lower red band represents holo-Fd (labeled Fd). A Coomassie stain of the native gel directly below illustrates that the protein levels in all of the experimental samples are the same. (C) The UV–vis absorption spectroscopy of the incubation samples before and after a 60 minute cluster transfer incubation, as above. The peaks of holo-Fd and of NAF-1 absorptions are marked (423 and 458 nm, respectively). (D) Replacement of a single-coordinating His114 in NAF-1 with Cys (H114C) shows no transfer to apo-Fd [29].

to mitochondria, cells were permeabilized by a short exposure to the mild surfactant digitonin to allow for the penetration of NEET proteins (Fig. 13B). The effect of NEET addition on RPA fluorescence was then measured with an Epi-fluorescent microscope. As a final assurance that all fluorescence is quenched, iron is added to the cells in the form of FeHQ ($FeCl_3$/8-hydroxyquinoline complex). Fig. 13A–B describes the experimental tools and work flow, and Fig. 13C–D shows a representative example of typical results using H9c2 rat cardiomyoblast cells. In this example the addition of NAF-1 led to the quenching of the RPA fluorescence in a concentration-dependent manner [23]. Similar results were obtained when mNT was added to HEK-293 cells [47]. However, the addition of the mutated proteins with four cysteines in the cluster binding site, H87C mNT mutant, or H114C NAF-1 mutant, did not result in quenching showing that they were not effective Fe/Fe–S donors to the mitochondria. These results show the importance of the unique 3Cys–1His coordination for Fe/Fe–S donation in cells [23,47] and are in agreement with the *in vitro* cluster transfer data described above. Additional cell biology tools used to study NEET function in cells included TMRE

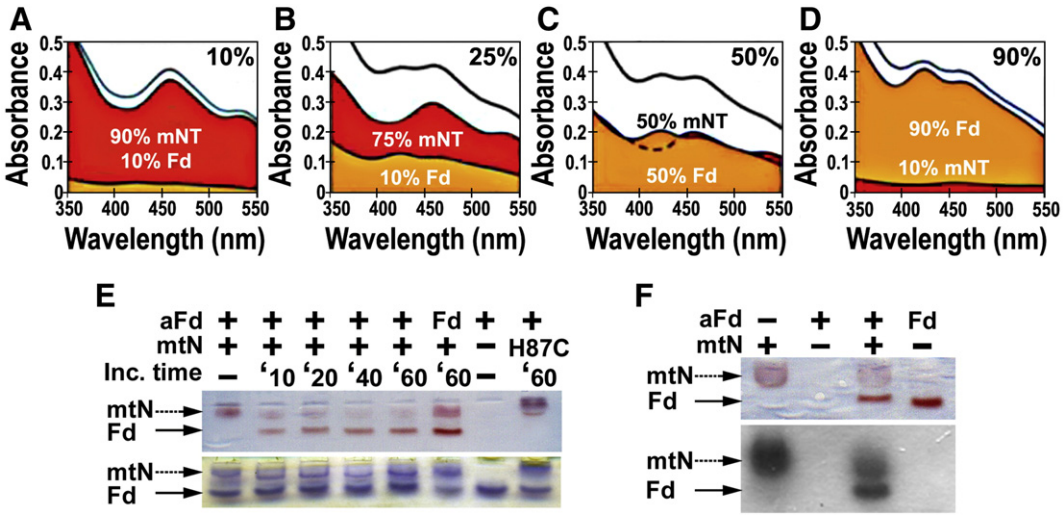

Fig. 12. Rates and quantification of cluster transfer from mNT to apo-Fd. The presence of the [2Fe–2S] cluster in mNT can be observed by UV–vis spectroscopy with a signature peak at 458 nm and in Fd at 423 nm. Frames A through D show the cluster transfer reaction progress (in the specified times). The observed spectra for the combined species are shown as a black line at the top of each frame while the deconvoluted spectra of holo-mNT (red) and holo-Fd (orange) are shown below. (D) Upon approaching completion, the visible spectrum resembles that of Fd, as all apo-Fd has been converted to the holo form and mNT has been converted to the visible-lacking apo form. The upper right corner in each spectrum indicates the percent completion for the cluster transfer reaction. (E) Transfer of mNT's (mtN) [2Fe–2S] cluster to apo-Fd (aFd) is also observed by Native-PAGE. Upon incubation with apo-Fd, mNT shows diminished color, indicating cluster loss over time as the [2Fe–2S] cluster is transferred to apo-Fd evident as a smaller molecular weight red-colored band indicating formation of holo-Fd. (F) In addition, ^{55}Fe-labeled mNT (mtN) was shown to transfer its cluster to apo-Fd (aFd) by Native-PAGE and radioactively detected [47].

(tetramethylrhodamine, ethyl ester) or DHE (dihydroethidium) for sensing changes in the levels of mitochondrial membrane potential (MMP), or reactive oxygen species (ROS), respectively upon disruption of NEET proteins' levels (see below) [51]. It should be noted that transfer of iron/cluster from NEET proteins to mitochondria upon addition of purified NEET proteins to permeabilized cells was used to demonstrate the ability of NEET proteins to donate their clusters in cells. As described below, a multitude of approaches was used in recent years in an attempt to decipher the biological function of NEET proteins.

3.3. The involvement of NEET proteins in key cellular process

3.3.1. NAF-1 is involved in autophagy regulation via interactions with Bcl-2

Different environmental conditions, such as hypoxia, nutrient starvation, or viral infection, as well as different developmental programs, can trigger several alternative pathways in cells including apoptosis, a form of programmed cell death, or autophagy, a pathway for cell survival that results in a selective degradation of cellular components and the recycling to basic building blocks and energy equivalents [52,53]. A basal level of autophagy is vital for homeostasis in the cell as nutrient supply fluctuates in the natural environment. Increased autophagy could occur for example during stress, caused by extracellular factors such as severe deficiency in nutrients, hypoxia, or accumulation of ROS, that leads to the accumulation of defective proteins and organelles. Due to their life-or-death decision role, apoptosis and autophagy are of course under strict cellular regulation. The control mechanisms on these processes involve large protein complexes that perceive signals from the cell and/or the environment and respond accordingly [54–57]. The NEET protein, NAF-1, along with Bcl-2 was shown to be part of one such complex, and NAF-1 was found to be necessary for the function of Bcl-2 in the control of autophagy at the ER [55]. Bcl-2's role in this control is to anchor the Beclin-1 complex, essential for the formation of the autophagosome, to the ER, thereby inhibiting autophagy. Bcl-2 does not bind the Beclin-1 complex when a member of the BH3-only protein family binds to it (Fig. 14B). It was suggested that NAF-1 along with the IP_3 receptor, a channel for calcium ions in the ER membrane, forms the foundation for Bcl-2 anchoring to the ER and to the Beclin-1 complex (Fig. 14A).

To obtain molecular details on the interaction between NAF-1 and Bcl-2, several functional assays were combined with binding assays and a novel use of a computational technique called *D*irect *C*oupling *A*nalysis (DCA). The advantage of including functional assays is that they are the ultimate indication that indeed binding has a functional consequence. The first use of such assays for deciphering the protein–protein interactions involving a NEET protein was reported in [58] in which we showed binding of Bcl-2 or Bcl-2 peptide(s) to NAF-1 and studied the effect of this binding on NAF-1's 2Fe–2S cluster stability and transfer [58].

The functional analysis of NAF-1 binding to Bcl-2 was complemented with two other experimental techniques to obtain a detailed map of these molecular interactions. One method was peptide array analysis which identifies peptide fragments from Bcl-2 to which NAF-1 binds. The second method used deuterium exchange mass spectrometry (DXMS) to identify parts of NAF-1 that exchange deuterium more slowly when incubated in D_2O upon binding of Bcl-2 and *vice versa*. Combined, these techniques indicated that NAF-1 binds to small segments of the BH3 and BH4 regions of Bcl-2 and to its disordered loop.

The different sets of experimental results were then combined with a new use of DCA which searches for co-evolved amino acids that are expected at protein–protein interfaces. Because each technique on its own has limitations and potential systematic errors, the combination of the different platforms provided an unprecedented level of detail for the interaction interface between NAF-1 and Bcl-2 that was not possible by any subset of techniques on their own. The combined approaches yielded the molecular Bcl-2-NAF-1 interaction map presented in (Fig. 14C–E) [58].

3.3.2. NEET proteins are involved in cellular and whole organism iron/ROS homeostasis

The involvement of the NEET proteins in cluster/iron transfer to mitochondria (Fig. 13) [23,47] hinted at a possible involvement of NEET proteins in cellular iron homeostasis. To explore this possibility at the *whole organism level*, studies were performed in the model plant *A. thaliana*, in which genetic manipulations are easily established and maintained, and phenotypic measurements are possible. *A. thaliana*

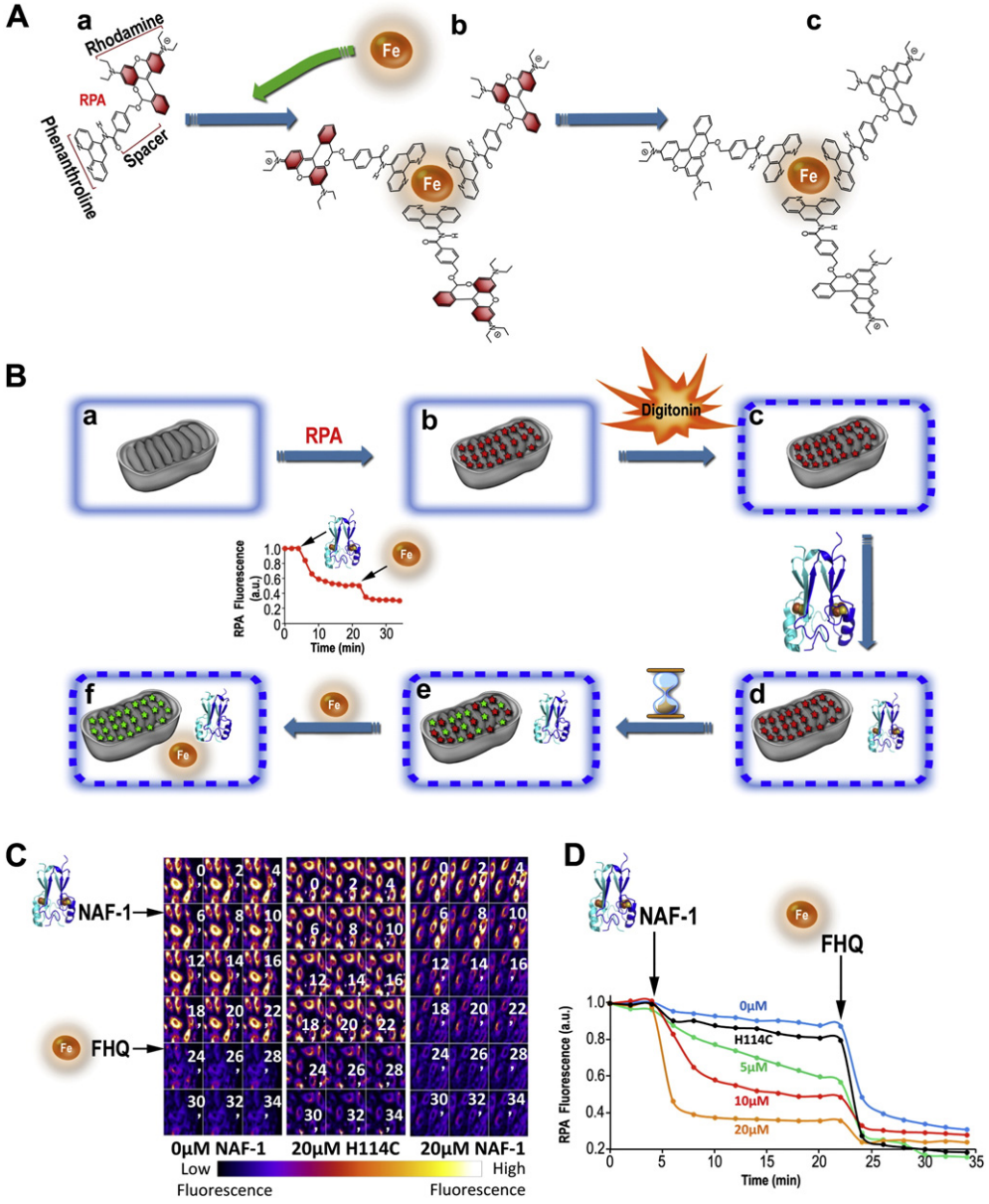

Fig. 13. Determination of mitochondrial iron levels upon addition of NEET proteins to permeabilized cells. *The experimental system*: (A) The RPA probe: (a) the chemical structure of RPA — the cationic fluorophore, rhodamine is conjugated to the iron chelator phenanthroline *via* aminocarbonyl benzylester. The red filled mitochondria indicate a highly fluorescent state. (b) The formation of RPA/Fe^{2+} complex with a stoichiometry 3:1 ratio. (c) Quenching of RPA upon binding with iron. (B) The cellular *in situ* system to analyze NAF-1 effects on mitochondrial iron levels: (a) a representative mitochondria in a cultured cell, (b) was stained with RPA (c) and the cultured cell was permeabilized using mild surfactant digitonin (d) intake of NAF-1 proteins by simple incubation with cultured cells. (e) The fluorescent change of RPA was monitored by microscopy over time. (f) The total quenching of RPA obtained using highly membrane permeant FeHQ. *Transfer of labile iron from NAF-1 to mitochondria*. (C) Pseudo-colored images of permeabilized H9c2 cells labeled with red RPA to trace iron in the mitochondrial matrix. Change in RPA fluorescence was measured every 2 min. NAF-1 (WT or H114C mutated) was added to concentrations of 0, 5, 10, or 20 μM after 4 min. The pseudocolor of the cells indicates the relative levels of mitochondrial RPA fluorescence (orange: high; blue: low). The highly membrane permeant FHQ was added after 22 min in order to attain maximum quenching. (D) Plot of RPA fluorescence (arbitrary units, a.u.) obtained by analyzing individual cell fluorescence with the ImageJ program. The RPA fluorescence is the average of four independent runs [23].

has the additional advantage that it contains only a single homologous NEET gene, At5g51720 (At-NEET) [31]. At-NEET was found to localize to the chloroplast and to the mitochondria [31,59]. Phenotypic characterization of At-NEET knockdown plants revealed a key role for this protein in plant development, senescence, reactive oxygen homeostasis, and Fe metabolism (Fig. 15). A role in Fe metabolism was further supported by biochemical and cell biology studies of At-NEET in plant and mammalian cells, as well as by mutational analysis of its cluster binding domain. Our findings support the hypothesis that NEET proteins have an ancient role in cells associated with Fe metabolism [31]. The results obtained in the plant system were essentially the same as those obtained in mammalian cells and mice in which the levels of the NEET proteins were decreased by either shRNA or gene knock out (KO) studies [51].

3.3.3. Interactions of mNT with proteins involved in cellular redox control

3.3.3.1. Thioredoxin/thioredoxin reductase. Recently, mNT was reported to interact with the *E. coli* thioredoxin/thioredoxin reductase system, demonstrating that these biological thiols can reduce the cluster of NEET proteins both *in vitro* and in the *E. coli* cellular environment [60]. It was reasoned that if mNT is reduced in *E. coli* cells which have a

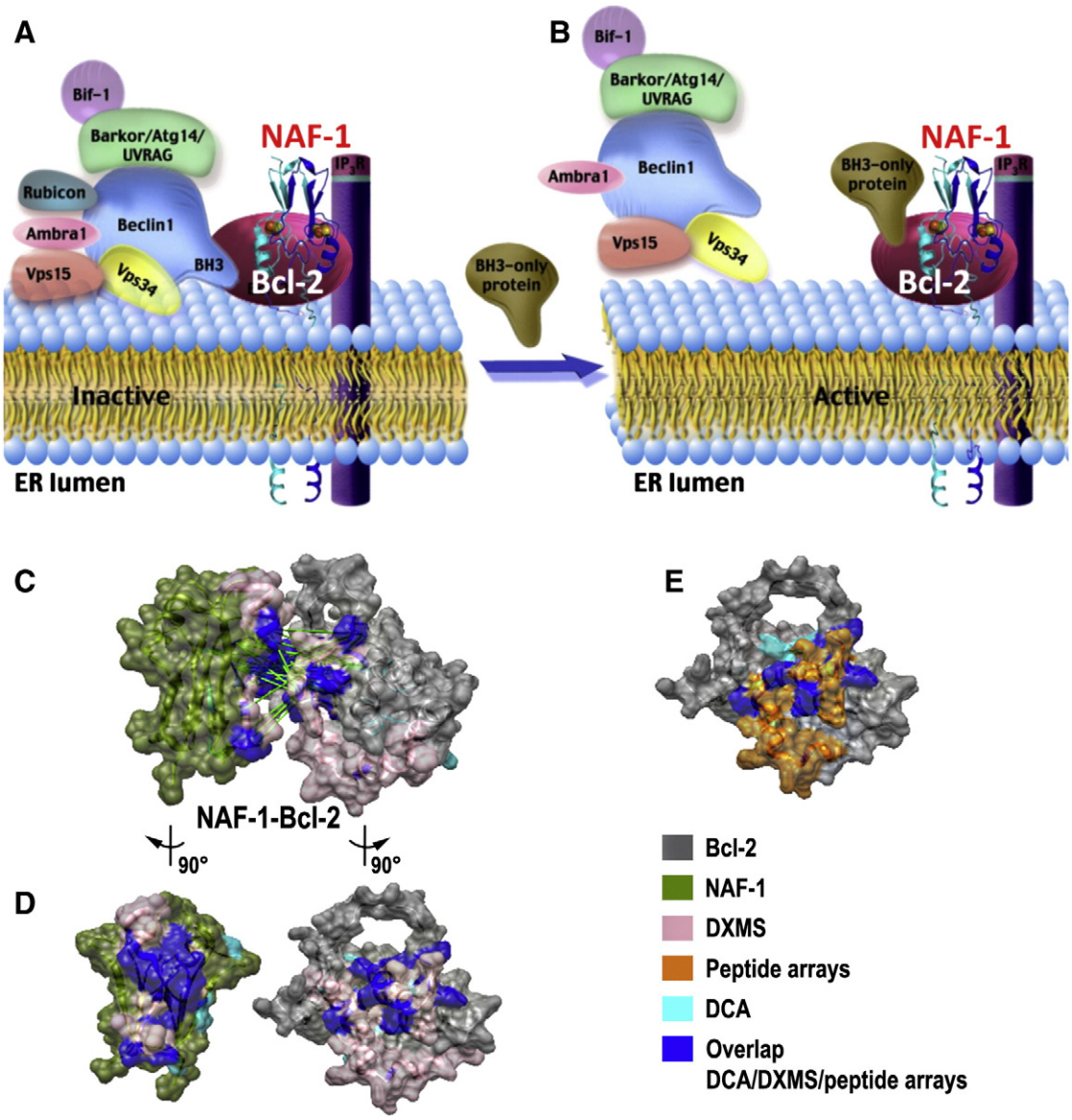

Fig. 14. Involvement of NAF-1 in autophagy. (A–B) Schematic model of the Beclin1/Bcl-2/NAF-1 complex and autophagy regulation at the ER. A simplified vision of the complex is shown before (A) and after autophagy induction (B). NAF-1 was found to be necessary for the activity of Bcl-2 in the control of autophagy at the ER. Bcl-2's role in this control is to anchor the Beclin-1 complex, essential for the formation of the autophagosome, to the ER thereby inhibiting autophagy. Bcl-2 does not bind the Beclin-1 complex when it is bound to another member of the BH3-only protein sub-group. It was suggested that NAF-1 along with the IP_3 receptor, a channel for calcium ions in the ER membrane, forms the foundation for Bcl-2 anchoring of the Beclin-1 complex to the ER (adopted from Maiuri et al. [57]). (C–D) *NAF-1–Bcl-2 molecular interactions*: Predicted interacting surface of NAF-1 and Bcl-2 using an experimental/theoretical integrated approach. (C) A putative interacting surface determined from DCA constraints (green links). The DXMS results showing all protected residues are highlighted in pink and dark blue. Dark blue is the overlap between DXMS and the top 30 couples determined using DCA. (D) NAF-1 and Bcl-2 are peeled apart and rotated by 90° as indicated. (E) Bcl-2 with interacting peptides from the array is shown in orange, and DCA residues are in cyan. Dark blue is the overlap between the peptide array and DCA. The combination of techniques provides a more detailed molecular model than is obtainable from any one technique on its own [58].

cytosolic redox potential of −260 mV, then it would likely be reduced at the lower redox potential of eukaryotic cells (typically −325 mV).

3.3.3.2. Glutamate dehydrogenase. A recent report showed a potential interaction between apo-mNT and glutamate dehydrogenase (GDH1) based on protein pull-down experiments using mNT as a bait [61]. mNT was found to form a covalent complex with GDH1 through disulfide bond formation. This bond required however the loss of the 2Fe–2S cluster from mNT. Upon complex formation, reduction of NAD^+ by GDH1 was accelerated by ~2-fold. The accelerated activity was lost upon reduction of the disulfide bond. The authors suggest that mNT (apo-mNT) acts as an allosteric modulator of GDH1, which is a mitochondrial enzyme with an important role in insulin secretion.

3.4. mNT is involved in inflammatory and metabolic diseases

Following the discovery of mNT by Colca et al. [17], describing the specific cross linking of mNT to thiazolidinedione (TZD), a type 2 diabetes drug, several other publications reported the pharmacokinetics of TZDs in relation to mNT [62–71]. TZDs are effective insulin-sensitizing drugs for the treatment of metabolic and inflammatory diseases, but their use is limited due to their side effects that are mediated by the ectopic activation of the peroxisome proliferator-activated receptor γ (PPARγ). Several TZD-based anti-diabetic drugs have been removed from the market due to these associated side effects. The connection of mNT to TZDs suggests that these drugs could act through modification of mitochondrial metabolism, preventing metabolic inflammation and allowing the up-regulation of mitochondrial biogenesis [72]. Mitochondrial activity and the etiology of obesity, insulin resistance and the

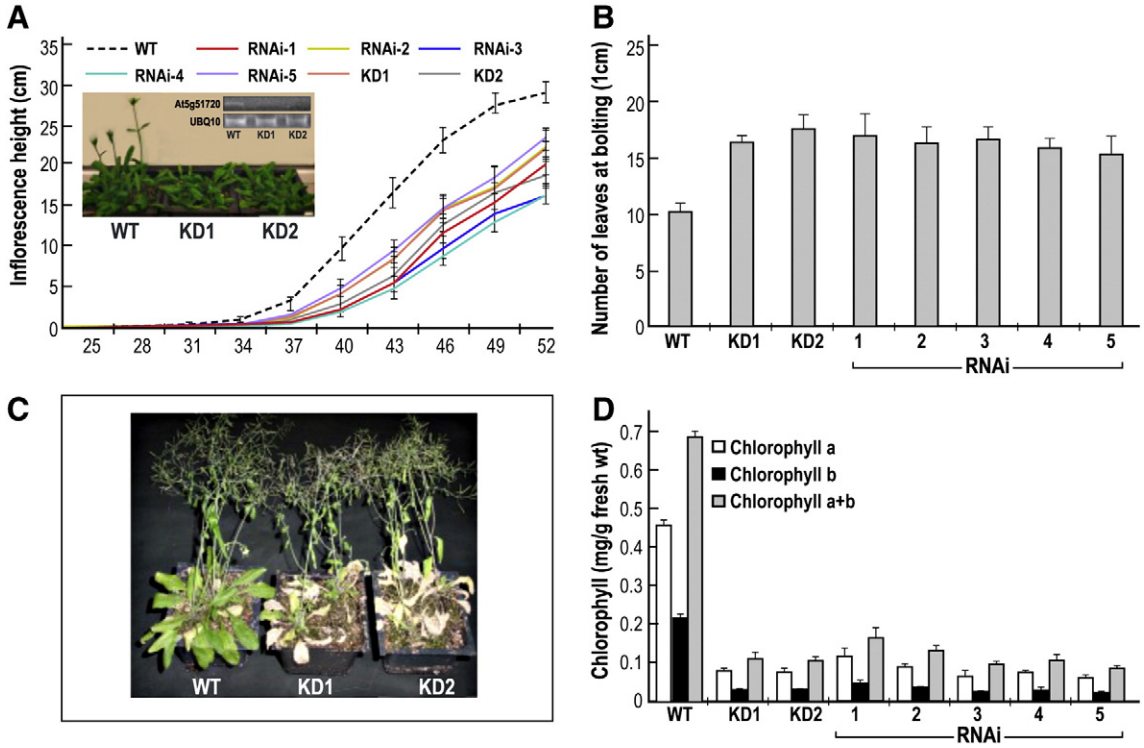

Fig. 15. Late bolting and early senescence phenotypes of *Arabidopsis* plants with suppressed expression of At-NEET. (A) Inflorescence height in the wild type (WT), knockdown plants, and RNAi lines for At-NEET. A representative photograph of 38-d-old wild type and two independent knockdowns for At-NEET is shown along with an RT-PCR gel for the expression of NEET in the plants photographed. (B) Leaf number at the time inflorescence height reached 1 cm in wild-type knockdown plants and RNAi lines for NEET. (C) Photograph of 58-d-old wild type and two independent NEET knockdowns grown under controlled growth conditions. (D) Chlorophyll content in wild-type knockdown plants and RNAi lines for NEET. Plants (58-d-old) were grown under controlled conditions in a mixed plot setting [31].

progression of type 2 diabetes were also attributed to mNT in a recent study showing that overexpression of mNT in adipocytes enhances lipid uptake and storage resulting in an expansion of the mass of adipose tissue [73]. Interestingly, overexpression of mNT in adipocytes of ob/ob diabetes model mice increased the uptake and storage of lipids in adipose tissue without a loss of insulin sensitivity [73]. This increased adipose lipid accumulation was accompanied by a reduction in ectopic lipid accumulation, which is associated with reduced insulin sensitivity. Increased adipocyte production of the lipid uptake-promoting hormone adiponectin was also observed. Mitochondrial iron levels were reduced in these mNT overexpressing cells, leading to a decrease in activity of the iron-dependent electron transport chain (ETC), lowering the rate of β-oxidation. With reduced mitochondrial respiration, lower levels of damaging ROS are produced. In addition to reducing iron transport into the matrix, mNT overexpression lowered mitochondrial membrane potential and oxidative damage, and led to higher production of adiponectin. The level of mNT expression was therefore found to markedly affect the dynamics of cellular and whole body lipid homeostasis [73].

Another recent study demonstrated the relationship between mNT and the inflammatory mediator TNF-α in liver cells [74]. Exposure of primary mouse hepatocytes to fructose and ethanol induced the overexpression of mNT, which primed the cells for TNF-α induced cytotoxicty. TNF-α induced the translocation of a Stat3–Grim-19 complex to the mitochondria, which bound mNT and promoted the rapid release of its 2Fe–2S cluster, causing iron accumulation that led to increased ROS resulting in mitochondrial injury and cell death. Further understanding of the relation of mNT to metabolism and inflammation, as well as the identification of additional drugs that bind NEET proteins could drive the development of future therapeutic strategies to treat metabolic and inflammatory diseases [75].

3.5. Interaction of the anti-type 2 diabetic drug pioglitazone and other small molecules with NEET proteins

Decreasing mNT protein levels in mice reduces mitochondrial respiration capacity. In heart cells of mNT knockout mice a decrease of 30% in oxygen consumption was observed in addition to a similar decrease in maximal uncoupler-stimulated respiration rate [18]. Damage to the mitochondria is often associated with resistance to insulin and the development of type 2 diabetes [76]. In recent years it was suggested that the pathogenesis of certain diseases lowers mitochondrial oxidation in insulin-resistant tissues. Drugs targeting insulin resistance, such as the TDZ pioglitazone, increase the oxidation capacity of cells [77,78] and suppress the activity of complex I in the mitochondrial respiration system [79].

As described above, mNT was initially identified as a cellular TZD (pioglitazone)-binding protein [17]. Upon mNT's isolation and crystallization, functional measurements showed that addition of pioglitazone stabilized the 2Fe–2S cluster of mNT [24]. Additionally, preferential binding of pioglitazone to the reduced state of mitoNEET was measured using protein film voltammetry [38]. Subsequently, a new cellular assay was developed which showed that pioglitazone inhibits iron/Fe–S transfer from mNT to the mitochondria [47]. In addition, high concentrations of pioglitazone were found to inhibit the interaction between the thioredoxin/thioredoxin reductase complex and mNT [60].

Binding of other small molecules to mNT was also investigated using a molecular blind docking method [66]. The results suggested a docking site for pioglitazone and identified potential novel target molecules for binding to mNT such as magnolol and enterobactin [66] (for review see Geldenhuys et al. [80]). Resveratrol-3-sulfate was shown recently to bind mNT [67]. The first structure-based drug-designed mNT-ligand was NL-1 [65,68] in which removal of the "tail" of pioglitazone

eliminated PPAR-γ binding activity without affecting mNT binding affinity. Additionally, NL-1 mildly uncoupled the mitochondrial gradient and was able to protect neuronal cells (N2A) against the electron transport complex I toxin rotenone [68,81].

A biological molecule that affects the properties of the 2Fe–2S cluster of mNT was first reported by Zhou and coworkers [82]. They found that mNT's cluster stability was decreased by the binding of the cellular redox regulator nicotinamide adenine dinucleotide phosphate (NADPH). They determined by NMR and mutagenesis that residues K55 and H58 were critical to this interaction. In addition to destabilizing the cluster, our group found that NADPH inhibits the transfer of the 2Fe–2S cluster to apo-acceptor proteins [69]. We determined a Ki of 0.2 mM for NADPH, which is in the physiological range for the concentration of this compound. These results suggest that NADPH is a cellular regulator of mNT 2Fe–2S cluster transfer to apo-acceptor proteins. Additionally, we found through mutagenesis that residue D84 in the CDGSH domain was necessary for the effect of NADPH binding on mNT cluster transfer function. This residue is highly conserved in orthologs across all kingdoms of life, suggesting that the interaction between mNT and NADPH might be of universal importance.

Pioglitazone and resveratrol, a small natural molecule that increases life span [68], were also recently shown to bind to NAF-1 [23]. These studies provided an explanation to the finding that pioglitazone could still bind to the mitochondria of mNT knock-out cells, presumably through binding to NAF-1 [71]. Incubation of NEET proteins with pioglitazone or resveratrol led to an increase in the stability of the 2Fe–2S cluster and inhibited the transfer of Fe/Fe–S from the protein to the mitochondria *in situ* [23,47]. Screening of the electrostatic environment by the addition of $MgCl_2$ resulted in a slight acceleration of cluster transfer from NAF-1 to the acceptor protein apo-Fd, and altering the hydrophobicity of the reaction conditions by the addition of glycerol dramatically inhibited the transfer. These results suggested an important role for hydrophobic residues in the interactions and docking of pioglitazone or resveratrol to NAF-1. Interestingly, the H114C mutant of NAF-1 was not affected by any of the compounds indicated above and their presence did not enable H114C to transfer its cluster to the acceptor protein [29,47].

3.6. mNT involvement in Cystic Fibrosis (CF)

Mutations in the *CFTR* gene (CFTR chloride channel) are known to cause the autosomic recessive disease Cystic Fibrosis (CF). mNT was discovered to be a CFTR-dependent gene since mNT mRNA was found to be down-regulated in cystic fibrosis cells and its level restored by ectopically expressing wt-CFTR in CF cells [83]. In addition, inhibition of CFTR's chloride transport activity resulted in down-regulation of mNT mRNA while CFTR stimulation upregulated mNT expression. CF has been shown to be associated with mitochondrial failure. The reduced expression of mNT in CF cells may induce a failure in the electron transport and oxidative phosphorylation of mitochondria thus contributing to the CF disease phenotype [83].

3.7. NEET protein involvement in early neural development and neurodegenerative diseases

Neurodegenerative diseases are often comprised of multiple disorders that lead to neuronal cell death. A screen to identify molecular markers for early neuronal development found two previously unknown transcripts, one of which (*Noxp70* transcript) is the mRNA coding for NAF-1 [19]. Using *in situ* hybridization it was also shown that NAF-1 was overexpressed in the brain. These findings revealed that *Noxp70* was strongly expressed at embryonic day 15, in the ventricular zone around the telencephalic ventricle, whereas lower expression was identified in the thalamus and hypothalamus. These results were first to suggest NAF-1 as a potentially important protein for neural development.

The neurodegenerative disease Parkinson's (PD) affects about 1% of the population over the age of 65. Mitochondrial integrity and function were shown to be key factors in maintaining normal, healthy cells, especially non-dividing ones, such as neurons. Recently, *PARKIN*, a causal gene for autosomal recessive early-onset parkinsonism, has been demonstrated to interact with mNT [84]. In several reports in which the discussion of possible drug targets for neurodegenerative diseases and CNS injury were discussed in relation to mitochondrial dysfunction, mNT was cited as a potential therapeutic approach for these diseases [81, 85,86].

3.8. NAF-1 is involved in disease, the genetic disorder WFS2, and longevity

A recessive mutation in *CISD2*, the gene encoding NAF-1, located on chromosome 4, leads to Wolfram Syndrome 2 (WFS2) [14,21,87]. This mutation is a point mutation – guanosine is replaced by cytosine – and as a result the second exon (out of three) in the NAF-1 pre-mRNA is skipped. The skipping of exon 2 changes the reading frame and thereby causes the formation of a premature termination codon in exon 3. In the mutated mRNA 75% of the protein sequence is not translated including the iron–sulfur cluster binding domain (Fig. 16). WFS2 patients suffer from diabetes, sight and hearing loss, nerve degeneration and a severe bleeding tendency [14,21,87].

In addition, the region of chromosome 4, where the gene encoding NAF-1 is located, hosts a number of genes associated with longevity [87,88]. A constitutive over-expression of NAF-1 in transgenic mice delays aging [89]. In contrast, knockout of NAF-1 in mice led to early aging and general health problems such as blindness, distortion of the skeleton, bleeding and muscle and nerve degeneration. In addition, serious damage to the mitochondria was observed along with an increase in autophagy [22] (Fig. 17). The latter symptoms are similar to those seen in WFS2 patients. Moreover, studies of NAF-1 knockout fibroblasts displayed ER stress and showed hallmarks of the unfolded protein response [16]. The studies described above point to a central role for

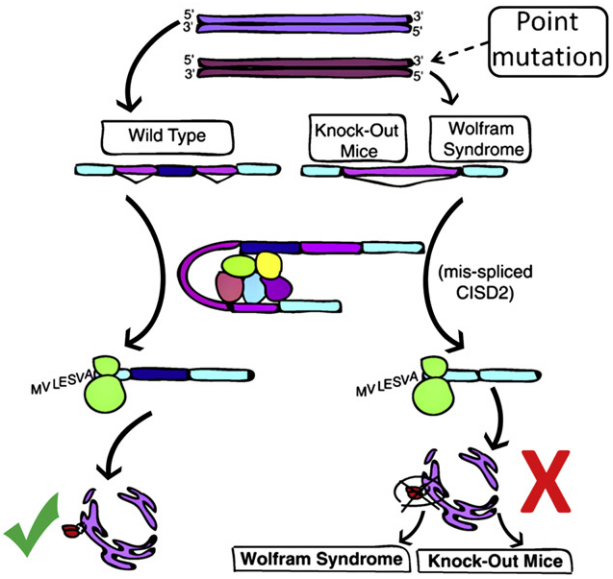

Fig. 16. Eliminating the function of NAF-1 leads to multiple symptoms in both human and mice models. The *CISD2* gene, shown at the top, codes for the OMM/ER protein NAF-1 (left-hand side). Wolfram Syndrome 2 (WFS2) is attributed to a single base pair conversion in the *CISD2* gene that results in a splicing error that completely eliminates exon 2, causes a frame shift and introduces a premature stop codon in exon 3 (right-hand side) [14]. For these reasons, 75% of the protein sequence is not translated, and no NAF-1 is properly assembled in the OMM and ER (lower part of the right-hand side). The absence of this protein causes a wide range of symptoms in WFS2 patients, including diabetes mellitus and optical atrophy. In an independent study, CISD2 knockout mice have similar symptoms (created based on Conlan et al. [21]).

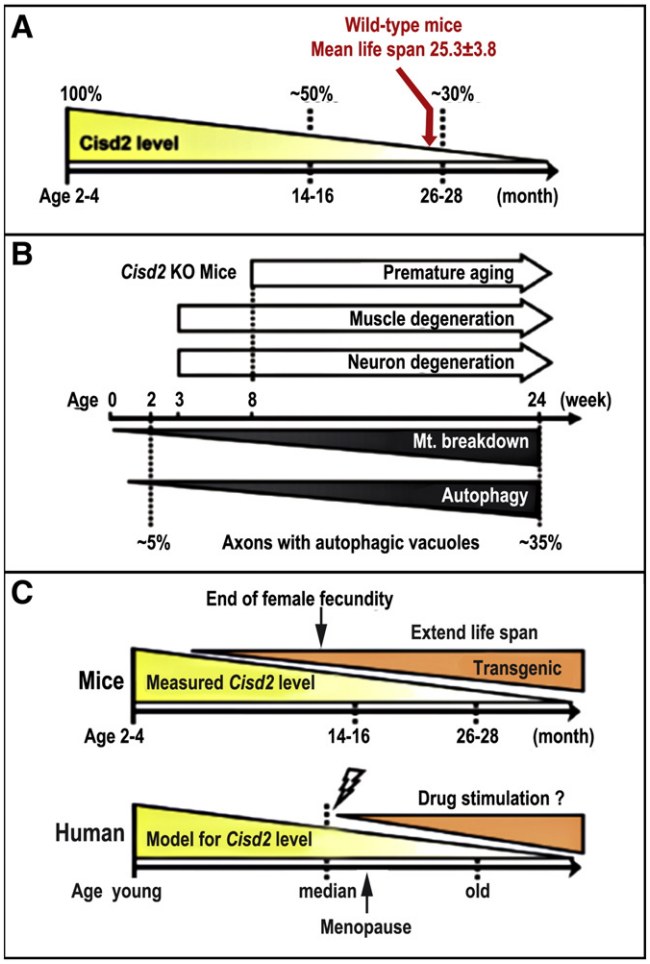

Fig. 17. NAF-1 (*Cisd2*) mediates mitochondrial integrity and is essential for mammalian life-span control. (A) The expression level of *CISD2* decreases in an age-dependent manner in naturally aged wild-type mice; there is an average 50% and 70% decrease in the 14–16 months old and 26–28 months old mice, respectively, compared to 2–4 months old young mice. In the wild-type mice, the mean life span is 25 ± 4 months. Partially disintegrated mitochondria that accompany autophagy induction were detected in aged mice. (B) In *CISD2* knockout mice, the mitochondrial outer membrane seems to break down prior to the destruction of the inner cristae. The damaged mitochondria appear to induce autophagy in order to eliminate the dysfunctional organelles. Importantly, mitochondrial (Mt) breakdown exacerbates with age and autophagy increases in parallel to the development of the premature aging phenotype in the *Cisd2* knockout mice. (C) Elevated levels of Cisd2 in transgenic mice or drug-stimulated expression in human may ameliorate aging phenotypes such as muscle and neuronal tissue degeneration and/or extend life span. Bearing in mind the evolutionary differences between rodents and humans, the response to increased Cisd2 may be different (created based on Chen et al. [22]).

NAF-1 in mediating key, life-or-death, cellular and developmental processes in mammals.

3.9. NEET proteins and cancer

Recently, a strong correlation was observed between the level of expression of NEET proteins and proliferation of various cancer cells, especially ones leading to the development of epithelial tumors. The expression of NEET mRNA was found to be elevated in many different types of cancer cells [90] with levels of mNT (*CISD1*) and NAF-1 (*CISD2*) mRNA expression elevated more than 40- and 140-fold, respectively, in breast cancer compared to normal cells [91].

NAF-1 and mNT protein levels were determined in three different epithelial breast cancer cell lines (MCF-7, MDA-MB-468 and HCC-70) compared to a non-cancerous breast epithelial cell line (MCF-10a). A substantial increase was found in the level of expression of NAF-1 in all cancerous cell lines and of mNT in two of the cancerous cell lines [51]. These findings are supported by experiments that measured the expression of mRNA encoding these NEET proteins in breast cancer

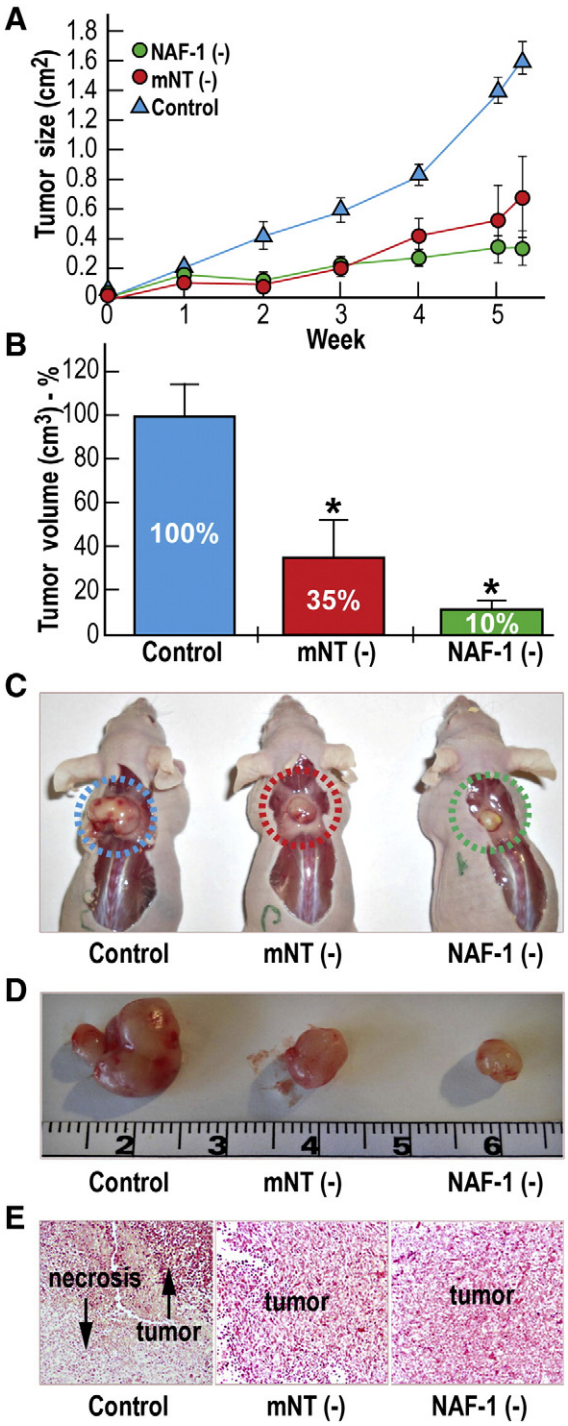

Fig. 18. shRNA of NEETs and tumor proliferation. NAF-1 or mNT is required to support tumor growth. Breast cancer cells (MDA-MB-231) with or without suppressed expression of mNT (mNT^{-}) or NAF-1 (NAF-1^{-}) were injected subcutaneously (s.c.) into the back of female CD1 nude mice, and tumor growth was monitored over time. (A) Slower tumor growth of breast cancer cells (MDA-MB-231) with suppressed expression of mNT (mNT^{-}) or NAF-1 (NAF-1^{-}) compared with control MDA-MB-231 cells. (B) Reduction of mean tumor volume expressed as percentage of control MDA-MB-231 in mNT^{-} or NAF-1^{-} MDA-MB-231 cells. (C and D) Images of representative tumors of each group obtained at the end of the experiment. (E) Histological analyses of tumors using H&E staining showing large necrotic areas in tumors formed from control MDA-MB-231 cells compared with tumors formed from mNT^{-} or NAF-1^{-} MDA-MB-231 cells. *$P < 0.05$ [51].

cells [90,92,93]. Salem et al. [93] suggested that NEET proteins encourage transformation and prevent autophagy in the mitochondria. They also showed that constitutive over-expression of mNT in breast cancer cells increases the size of the tumors developed from these cells [93]. We recently showed that knockdown of mNT or NAF-1 expression using shRNA, a common methodology to determine the biological function of proteins, decreased cell proliferation and tumor development of human epithelial breast cancer cells (Fig. 18) [51]. Several aspects of mitochondrial function were affected in cells with suppressed expression of mNT or NAF-1. These included a decrease in membrane potential, an increase in iron and ROS accumulation in mitochondria, a decrease in aerobic respiration and an increase in glycolysis. In addition, cells with suppressed expression of mNT or NAF-1 exhibited distorted mitochondrial structure as evident by abnormal elongation and loss of cristae (inner membranes) structures, and the accumulation of autophagosomes [51]. The different effects of lower NEET expression on the mitochondrial structure and function are schematically presented (Fig. 19), some of these, *e.g.* mitochondrial iron accumulation, are consistent with phenotypes observed when the levels of proteins involved in iron/iron–sulfur biogenesis and managements are decreased [49,50]. The appearance of autophagosomes was also accompanied by accumulation of proteins involved in autophagy suggesting that this process was triggered in cells with reduced expression of mNT or NAF-1 [51].

4. Outlook for the future of NEET protein research

NEET proteins such as mNT, NAF-1 and At-NEET were shown to be involved in many cellular processes, including calcium and iron homeostasis, mitochondrial function, mitigation of oxidative stress, and autophagy/apoptosis regulation [16,31,51,56]. Collectively these processes can affect a wide spectrum of cellular activities and improve the overall health of the organism. Indeed, the involvement of NEET proteins in numerous human diseases was described in detail in Section 2 above and is schematically summarized in Fig. 20.

Although our knowledge of NEET protein structure–function relationship has improved significantly since their discovery, many questions related to NEET protein function(s) remain unanswered. Among them are: What proteins in the cell donate their 2Fe–2S clusters to NEET proteins? What proteins accept their clusters from NEET proteins? What cellular transcripts, proteins and pathways respond to changes in mNT and/or NAF-1 protein levels? What metabolic processes are regulated by mNT and NAF-1? How do these processes change with the redox state of the cell and/or environmental *e.g.* nutrient stress?

The outlook for future research on NEET proteins is therefore broad and promising, and much remains to be learned about their biochemical and biological function(s), as well as their relation to human health and disease. One promising approach is the continued search for their cellular partners by experimental biochemical methodologies such as co-immunoprecipitation pull-down methods [55], peptide arrays [58,94,95], and yeast-2-hybrid assays [92]. These experimental approaches could now be complemented by new and novel computational techniques such as DCA, developed to identify and predict protein–protein interactions with a goal of suggesting partner proteins. We believe that the combination of experimental and computational techniques will provide an unprecedented level of detail which could be exploited for NEET protein investigations, as well as the design of therapies/drugs for NEET-related diseases.

Another promising avenue of experimental research is the use of different "omics" tools such as transcriptomics, metabolomics and proteomics. These methods could be applied to cells with altered expression of different NEET proteins, or to cells treated with different drugs that target NEET proteins, to identify and dissect the different pathways and metabolites/genes/proteins that are affected or linked to NEET proteins and their emerging interacting protein and metabolic networks.

Together, a synergy of experimental and theoretical approaches, as well as the use of a systems biology approach, will lead to a mechanistic understanding of NEET protein function in cells as well as their involvement in different human pathologies. Some of the different platforms to be used in future NEET research and their potential importance are outlined below.

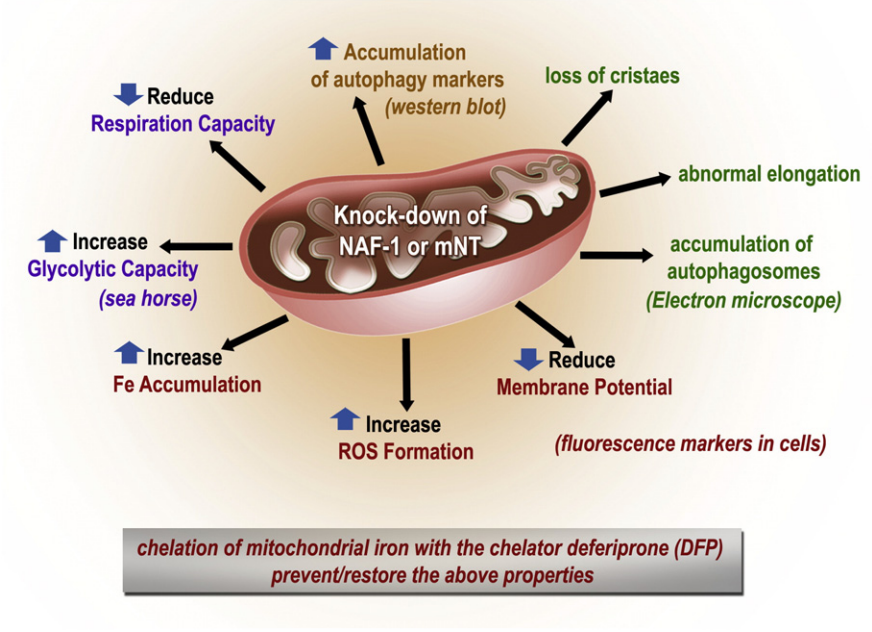

Fig. 19. Mitochondrial function in cells with low expression of NEET proteins. Culture cells with decreased expression of NEET proteins (mNT^{-} or $NAF\text{-}1^{-}$) showed decrease in membrane potential and an increase in the accumulation of iron and reactive oxygen species (ROS); determined from mitochondrial and ROS selective fluorescence measurements. These phenomena are mitigated by the addition of an iron chelator (red). Knockdown of mNT or NAF-1 also showed a decrease in aerobic respiration and increase glycolysis (purple); measured using the Seahorse Extracellular Flux Analyzer. Additionally, knockdowns showed mitochondrial physiology distortions reflected in the abnormal progressive lengthening and loss of cristae (green); measured using electron microscopy. Electron microscopy also revealed autophagosome accumulation in the knockdown cells. This interpretation was supported by western blots that showed an increase in the accumulation of autophagy markers (green and orange, respectively).

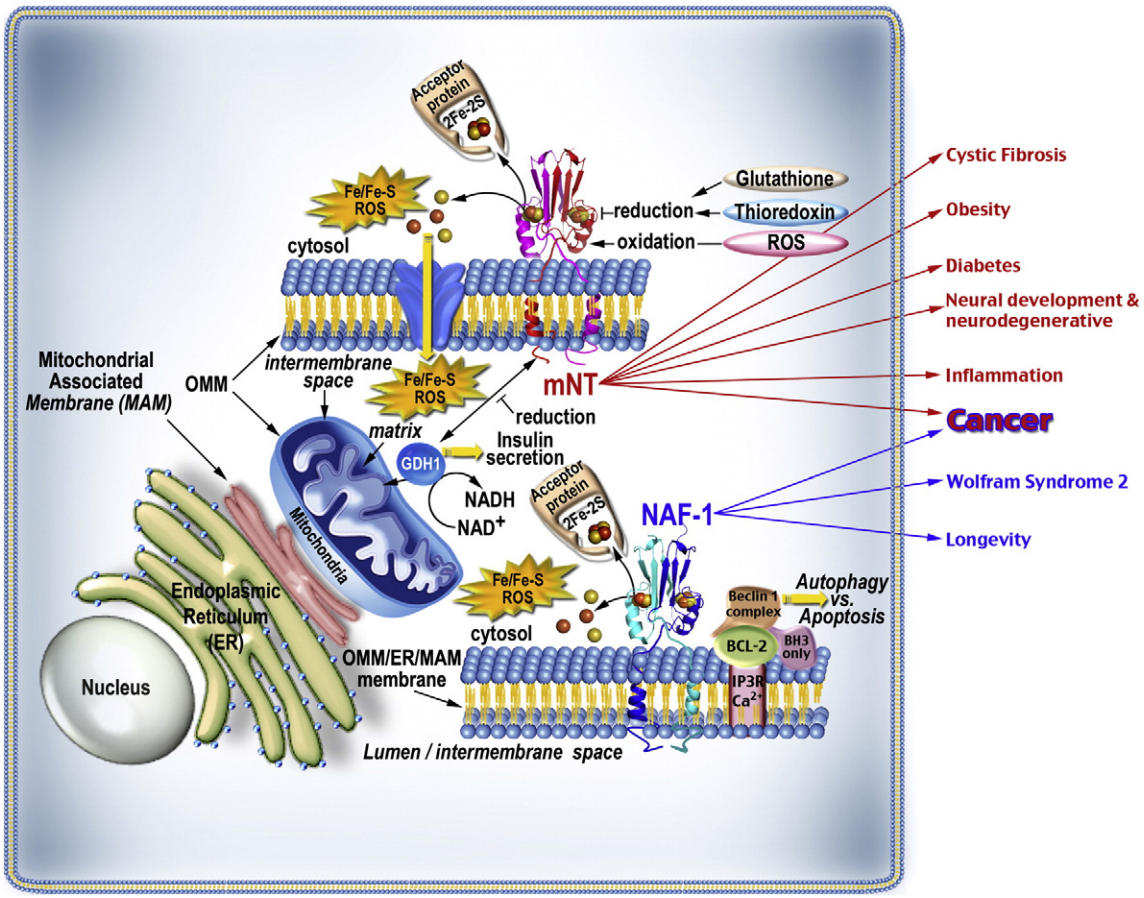

Fig. 20. Cellular localization, protein partners and function of the NEET proteins mNT and NAF-1, and the human diseases they are involved in. A scheme summarizing most of the research findings pertained to the function of NEET proteins. The mechanism of cluster loss, resulting in cluster transfer or alternatively cluster dissociation is illustrated as one of the key features of NEET protein function. This process leads in some cases to the enhanced generation of reactive oxygen species (ROS). Known putative protein partners and interacting molecules are specified. Genetic disorders or other disruption of the function and/or alteration of the cellular protein level of mNT or NAF-1 is shown to lead to different diseases.

4.1. NEET protein involvement in metabolic pathways in cells

Currently, the extent of changes to the global metabolite and gene networks in cells with altered NEET function is unknown. Metabolomics and transcriptomics tools will aid in characterizing the role of NEET proteins in the cell by revealing how the cellular chemistry and gene expression profile changes in response to NEET expression/modification.

i. Role of the NEET proteins in cellular regulation: RNA-Seq studies
A cell's transcriptome comprises all of the expressed RNA sequences, taking into account transcript structure, splicing and quantity. Technologies developed to determine the transcriptome include hybridization-based approaches, such as microarrays, and sequence-based approaches known as RNA-sequencing (RNA-Seq) (reviewed in [96,97]). Both technologies have been used extensively throughout the study of human diseases to better understand the transcriptional landscape of cellular aberrations [92,98–100]. Currently, RNA-Seq is the preferred method for measuring a cell's transcriptome, since it is able to measure absolute quantity of almost all transcripts in the cell, it accounts for alternative splicing and alternative start and stop sites, and it is able to detect different epigenetic regulatory mechanisms [96].
As described above, NEET proteins appear to play multiple roles in cells that could be dependent on specific cell function(s), energetic programming and the state of the cellular environment. Examples include the study of obesity in a model "pink" mice, the Wolfram model mice, NEET suppression in breast cells and tumors, as well as sustained longevity in NAF-1 overexpressing mice [9,16,19,22,51,64,73,81,83,85,86,89,100,101]. NAF-1 and mNT are implicated in affecting iron and calcium homeostasis, ROS accumulation and oxidative capacity, all of which are known effectors of nuclear and mitochondrial gene expression. RNA-Seq would be a key tool in determining whether NEET proteins directly activate/deactivate transcriptional regulators or alter the cellular environment triggering changes in gene expression. This information will aid in gaining a greater understanding of the specific mechanisms of NEET protein function.

ii. Role of the NEET proteins in cellular biochemistry: Metabolomics studies
Metabolomics is the study of metabolites accumulated in cells during different cellular processes. Metabolic profiling in a clinical or research setting, consisting of chromatography, ionization and mass spectrometry tools, has many applications, including determining the complete chemical profile of a cell or tissue, identifying altered proteins and protein complexes, and discovering and screening for disease-related chemical biomarkers in tissue and fluid samples. There are many excellent reviews discussing metabolic profiling tools, their application to analyzing human disease states and bioinformatics resources (review examples — [102–106]). NAF-1 and mNT are capable of transferring Fe–S clusters to recipient protein(s), possibly altering function, participate in iron and calcium homeostasis, cause energetic reprogramming and play a role in regulation of oxidative stress and

autophagy/apoptosis signaling. Modification of all of these processes is likely to cause changes in cells resulting in perturbations in cellular chemistry in cells with altered NEET protein expression. Metabolomics analysis will assist in understanding those perturbations. Several studies have used various metabolic profiling tools to analyze pathways related to diseases characterized by ER stress and mitochondrial dysfunction. Cross-referencing data drawn from related ER, mitochondria, oxidative stress and cancer studies with NEET specific metabolomics will support efforts to understand complex phenotypes observed in cells defective in NEET function.

Taken together, metabolomics and transcriptomics data yields a much more comprehensive snapshot of what is happening in the cell than either one alone. These coupled with proteomics tools will be instrumental in the future characterization of NEET proteins.

4.2. Protein–protein interactions: further development of DCA

The recent study of Tamir et al. [58] on the molecular interactions between Bcl-2 and the NEET protein NAF-1 clearly demonstrated the power of integrated experimental and theoretical approaches. In the latter, the DCA method was applied. This methodology has been useful to uncover pairwise amino acid dependencies, created through the course of evolution, which are embedded in sequences belonging to a protein family. These dependencies or couplings were shown to be a proxy of physical interactions among residue pairs within a protein [107]. Although intradomain residue–residue interactions is the most likely category of coupled sites, some very interesting exceptions were revealed which captured residue contacts, arising from alternative protein conformations, ligand-mediated residue couplings, and interdomain interactions in protein oligomers [107]. This methodology has been successful in the area of protein structure prediction [108,109] and has been useful to uncover conformational diversity in proteins [110,111]. However, its application to protein interactions seems to be more promising and already has shown interesting results [58,112,113]. DCA for protein interactions advances the idea that, just as in the case of intraprotein residue interactions, important inter-protein residue interactions coevolved and are maintained during evolution. As spontaneous changes occur in one partner protein, there exists an evolutionary drive to revert or select for compensatory changes on the partner protein. Information on these compensatory changes is contained within the sequences of protein domains in the diversity of nature. For the Bcl-2–NAF-1 interaction a few highly ranked couplings were structurally distant from the majority suggesting possible allosteric effects, which had previously been noted in that region of the protein [42].

To uncover the interaction network of NEET proteins, DCA could be used to propose interactions based on the ever-increasing availability of genomic sequences. The method could potentially identify key interaction sites between NAF-1 and other partner proteins, as well as between mNT and their partner proteins. These key interactions can be combined with molecular dynamics simulations such as Structure Based Models (SBM) [114,115] to predict high-resolution complex structures and identify important interaction interfaces. The use of DCA to study protein interactions in the NEET pathway is not limited to finding key interactions; the power of this theoretical tool also lies in the ability to do *in silico* mutagenesis in the proposed interacting partners and has a quantitative estimate of its effect on the interaction. An example of this for the case of two-component systems is documented in [113]. This strategy could potentially be used in the design of drugs or therapies directed at altering the interactions of NEET proteins with different cellular targets.

5. Summary

MitoNEET, originally identified as the mitochondrial target of the anti-diabetic TZD class of drugs, is the founding member of a small but distinct class of human redox active 2Fe–2S proteins, the NEET family. Representative members of NEET proteins were found in most other organisms, including archea, bacteria, algae, and plants demonstrating an evolutionary-conserved function. Biochemical and biophysical characterization showed that NEET proteins have unique properties that include a novel structure and ability to tune the redox potential of their clusters, a rare capability to transfer their 2Fe–2S clusters to other proteins, and a potential to transfer their cluster/iron to the mitochondria or chloroplast. Functional analysis in different biological systems demonstrated a role for NEET proteins in the regulation of ROS and iron homeostasis. Accordingly, misregulation or knockdown of these proteins leads to various health issues and missplicing of NAF-1 is a causative of Wolfram Syndrome 2. Both mNT and NAF-1 were found to be "enslaved" proteins in breast cancer cells, supporting cell proliferation and enhancing mitochondrial function of cancer cells. Knockdown of these proteins was therefore found to decrease growth of tumors in mice models. MitoNEET was found to associate with several proteins, including GDH1, which might link mNT back to its original identification as an anti-diabetic drug target. In addition, mNT was recently proposed to be involved in iron–sulfur biogenesis and trafficking [116]. NAF-1 associations with a distinct set of proteins include Bcl-2 linking NAF-1 to longevity, autophagy and apoptosis. Recently, genetic studies in Drosophila and human cells suggested two novel proteins (PPT1 and CLN3) as interactors of NAF-1 (CISD2) [88]. The ability to transfer the 2Fe–2S cluster in its entirety and without loss has only been observed in proteins involved in cluster assembly or transfer. Therefore, the findings that mNT and NAF-1 can satisfy those conditions suggest their involvement in cluster assembly/transfer processes, yet the physiological NEET cluster donor as well as apo-acceptors protein(s) need to be identified. Moreover, how is the function of cluster transfer related to the many diseases associated with NEET proteins is a subject for future investigations.

Although much has been learned over the decade about NEET proteins, as described above, many questions remain unanswered. We believe that a combination of several different complementary platforms that include theoretical, computational and experimental techniques will be needed to decipher the full range of biological functions and partner proteins associated with NEET proteins. Such an understanding will lead to the development of new drugs that target these important proteins and improve our chances of fighting several major health conditions such as cancer, diabetes, obesity and longevity, linked to NEET proteins.

Acknowledgements

This work is supported by the Israeli Science Foundation (ISF865/13) (to R.N.) and the National Institutes of Health (grants GM54038 and GM101467, to P.A.J.). R.N. is a member of the MINERVA Center for Biohybrid Complex Systems and acknowledges funds received from the Center.

References

[1] H. Beinert, Iron–sulfur proteins: ancient structures, still full of surprises, J. Biol. Inorg. Chem. 5 (2000) 2–15.
[2] H. Beinert, R.H. Holm, E. Münck, Iron–sulfur clusters: nature's modular, multipurpose structures, Science 277 (1997) 653–659.
[3] R. Lill, Function and biogenesis of iron–sulphur proteins, Nature 460 (2009) 831–838.
[4] R. Lill, U. Mühlenhoff, Maturation of iron–sulfur proteins in eukaryotes: mechanisms, connected processes, and diseases, Annu. Rev. Biochem. 77 (2008) 669–700.
[5] R. Lill, U. Mühlenhoff, Iron–sulfur protein biogenesis in eukaryotes: components and mechanisms, Annu. Rev. Cell Dev. Biol. 22 (2006) 457–486.
[6] S. Bandyopadhyay, K. Chandramouli, M.K. Johnson, Iron–sulfur cluster biosynthesis, Biochem. Soc. Trans. 36 (2008) 1112–1119.
[7] O. Stehling, C. Wilbrecht, R. Lill, Mitochondrial iron–sulfur protein biogenesis and human disease, Biochimie 100 (2014) 61–77.
[8] X.M. Xu, S.G. Møller, Iron–sulfur cluster biogenesis systems and their crosstalk, Chembiochem 9 (2008) 2355–2362.
[9] L.K. Beilschmidt, H.M. Puccio, Mammalian Fe–S cluster biogenesis and its implication in disease, Biochimie 100 (2014) 48–60.

[10] H. Ye, T.A. Rouault, Human iron–sulfur cluster assembly, cellular iron homeostasis, and disease, Biochemistry 49 (2010) 4945–4956.
[11] T.A. Rouault, W.H. Tong, Iron–sulfur cluster biogenesis and human disease, Trends Genet. 24 (2008) 398–407.
[12] F. Mochel, M.A. Knight, W.H. Tong, D. Hernandez, K. Ayyad, T. Taivassalo, P.M. Andersen, A. Singleton, T.A. Rouault, K.H. Fischbeck, R.G. Haller, Splice mutation in the iron–sulfur cluster scaffold protein ISCU causes myopathy with exercise intolerance, Am. J. Hum. Genet. 82 (2008) 652–660.
[13] C. Camaschella, A. Campanella, L. De Falco, L. Boschetto, R. Merlini, L. Silvestri, S. Levi, A. Iolascon, The human counterpart of zebrafish *shiraz* shows sideroblastic-like microcytic anemia and iron overload, Blood 110 (2007) 1353–1358.
[14] S. Amr, C. Heisey, M. Zhang, X.J. Xia, K.H. Shows, K. Ajlouni, A. Pandya, L.S. Satin, H. El-Shanti, R. Shiang, A homozygous mutation in a novel zinc-finger protein, ERIS, is responsible for Wolfram syndrome 2, Am. J. Hum. Genet. 81 (2007) 673–683.
[15] L. Rigoli, C. Di Bella, Wolfram syndrome 1 and Wolfram syndrome 2, Curr. Opin. Pediatr. 24 (2012) 512–517.
[16] S.E. Wiley, A.Y. Andreyev, A.S. Divakaruni, R. Karisch, G. Perkins, E.A. Wall, P. van der Geer, Y.F. Chen, T.F. Tsai, M.I. Simon, B.G. Neel, J.E. Dixon, A.N. Murphy, Wolfram syndrome protein, Miner1, regulates sulphydryl redox status, the unfolded protein response, and Ca2+ homeostasis, EMBO Mol. Med. 5 (2013) 904–918.
[17] J.R. Colca, W.G. McDonald, D.J. Waldon, J.W. Leone, J.M. Lull, C.A. Bannow, E.T. Lund, W.R. Mathews, Identification of a novel mitochondrial protein ("mitoNEET") cross-linked specifically by a thiazolidinedione photoprobe, Am. J. Physiol. Endocrinol. Metab. 286 (2004) E252–E260.
[18] S.E. Wiley, A.N. Murphy, S.A. Ross, P. van der Geer, J.E. Dixon, MitoNEET is an iron-containing outer mitochondrial membrane protein that regulates oxidative capacity, Proc. Natl. Acad. Sci. U. S. A. 104 (2007) 5318–5323.
[19] M. Boucquey, E. De Plaen, M. Locker, A. Poliard, S. Mouillet-Richard, T. Boon, O. Kellermann, *Noxp20* and *Noxp70*, two new markers of early neuronal differentiation, detected in teratocarcinoma-derived neuroectodermic precursor cells, J. Neurochem. 99 (2006) 657–669.
[20] S.E. Wiley, M.L. Paddock, E.C. Abresch, L. Gross, P. van der Geer, R. Nechushtai, A.N. Murphy, P.A. Jennings, J.E. Dixon, The outer mitochondrial membrane protein mitoNEET contains a novel redox-active 2Fe–2S cluster, J. Biol. Chem. 282 (2007) 23745–23749.
[21] A.R. Conlan, H.L. Axelrod, A.E. Cohen, E.C. Abresch, J. Zuris, D. Yee, R. Nechushtai, P.A. Jennings, M.L. Paddock, Crystal structure of Miner1: the redox-active 2Fe–2S protein causative in Wolfram syndrome 2, J. Mol. Biol. 392 (2009) 143–153.
[22] Y.F. Chen, C.H. Kao, Y.T. Chen, C.H. Wang, C.Y. Wu, C.Y. Tsai, F.C. Liu, C.W. Yang, Y.H. Wei, M.T. Hsu, S.F. Tsai, T.F. Tsai, Cisd2 deficiency drives premature aging and causes mitochondria-mediated defects in mice, Genes Dev. 23 (2009) 1183–1194.
[23] S. Tamir, J.A. Zuris, L. Agranat, C.H. Lipper, A.R. Conlan, D. Michaeli, Y. Harir, M.L. Paddock, R. Mittler, Z.I. Cabantchik, P.A. Jennings, R. Nechushtai, Nutrient-deprivation autophagy factor-1 (NAF-1): biochemical properties of a novel cellular target for anti-diabetic drugs, PLoS ONE 8 (2013) e61202.
[24] M.L. Paddock, S.E. Wiley, H.L. Axelrod, A.E. Cohen, M. Roy, E.C. Abresch, D. Capraro, A.N. Murphy, R. Nechushtai, J.E. Dixon, P.A. Jennings, MitoNEET is a uniquely folded 2Fe 2S outer mitochondrial membrane protein stabilized by pioglitazone, Proc. Natl. Acad. Sci. U. S. A. 104 (2007) 14342–14347.
[25] J. Lin, T. Zhou, K. Ye, J. Wang, Crystal structure of human mitoNEET reveals distinct groups of iron sulfur proteins, Proc. Natl. Acad. Sci. U. S. A. 104 (2007) 14640–14645.
[26] X. Hou, R. Liu, S. Ross, E.J. Smart, H. Zhu, W. Gong, Crystallographic studies of human mitoNEET, J. Biol. Chem. 282 (2007) 33242–33246.
[27] D.J. Ferraro, L. Gakhar, S. Ramaswamy, Rieske business: structure–function of Rieske non-heme oxygenases, Biochem. Biophys. Res. Commun. 338 (2005) 175–190.
[28] A.R. Conlan, M.L. Paddock, H.L. Axelrod, A.E. Cohen, E.C. Abresch, S. Wiley, M. Roy, R. Nechushtai, P.A. Jennings, The novel 2Fe–2S outer mitochondrial protein mitoNEET displays conformational flexibility in its N-terminal cytoplasmic tethering domain, Acta Crystallogr. Sect. F: Struct. Biol. Cryst. Commun. 65 (2009) 654–659.
[29] S. Tamir, Y. Eisenberg-Domovich, A.R. Conlan, J.T. Stofleth, C.H. Lipper, M.L. Paddock, R. Mittler, P.A. Jennings, O. Livnah, R. Nechushtai, A point mutation in the [2Fe–2S] cluster binding region of the NAF-1 protein (H114C) dramatically hinders the cluster donor properties, Acta Crystallogr. D Biol. Crystallogr. 70 (2014) 1572–1578.
[30] J. Lin, L. Zhang, S. Lai, K. Ye, Structure and molecular evolution of CDGSH iron–sulfur domains, PLoS ONE 6 (2011) e24790.
[31] R. Nechushtai, A.R. Conlan, Y. Harir, L. Song, O. Yogev, Y. Eisenberg-Domovich, O. Livnah, D. Michaeli, R. Rosen, V. Ma, Y. Luo, J.A. Zuris, M.L. Paddock, Z.I. Cabantchik, P.A. Jennings, R. Mittler, Characterization of *Arabidopsis* NEET reveals an ancient role for NEET proteins in iron metabolism, Plant Cell 24 (2012) 2139–2154.
[32] M.M. Dicus, A. Conlan, R. Nechushtai, P.A. Jennings, M.L. Paddock, R.D. Britt, S. Stoll, Binding of histidine in the (Cys)3(His)1-coordinated [2Fe–2S] cluster of human mitoNEET, J. Am. Chem. Soc. 132 (2010) 2037–2049.
[33] T. Iwasaki, R.I. Samoilova, A. Kounosu, D. Ohmori, S.A. Dikanov, Continuous-wave and pulsed EPR characterization of the [2Fe–2S](Cys)3(His)1 cluster in rat mitoNEET, J. Am. Chem. Soc. 131 (2009) 13659–13667.
[34] D. Bäckström, M. Lorusso, K. Anderson, A. Ehrenberg, Characterization of the iron–sulfur protein of the mitochondrial outer membrane partially purified from beef kidney cortex, Biochim. Biophys. Acta 502 (1978) 276–288.
[35] H.G. Heidrich, S.P. Albracht, D. Bäckström, Two iron–sulfur centers in mitochondrial outer membranes from beef heart as prepared by free-flow electrophoresis, FEBS Lett. 95 (1978) 314–318.
[36] T.F. Tirrell, M.L. Paddock, A.R. Conlan, E.J. Smoll Jr., R. Nechushtai, P.A. Jennings, J.E. Kim, Resonance Raman studies of the (His)(Cys)3 2Fe–2S cluster of mitoNEET: comparison to the (Cys)4 mutant and implications of the effects of pH on the labile metal center, Biochemistry 48 (2009) 4747–4752.
[37] C. Homer, D. Yee, H.L. Axelrod, A.E. Cohen, E.C. Abresch, C. Chang, R. Nechushtai, P.A. Jennings, M.L. Paddock, Structural basis for phosphate stabilization of the uniquely coordinated 2Fe–2S cluster of the outer mitochondrial membrane protein mitoNEET, Biophys. J. 96 (2009) 442a–443a.
[38] D.W. Bak, J.A. Zuris, M.L. Paddock, P.A. Jennings, S.J. Elliott, Redox characterization of the FeS protein mitoNEET and impact of thiazolidinedione drug binding, Biochemistry 48 (2009) 10193–10195.
[39] D.W. Bak, S.J. Elliott, Alternative FeS cluster ligands: tuning redox potentials and chemistry, Curr. Opin. Chem. Biol. 19C (2014) 50–58.
[40] D.W. Bak, S.J. Elliott, Conserved hydrogen bonding networks of mitoNEET tune Fe–S cluster binding and structural stability, Biochemistry 52 (2013) 4687–4696.
[41] J.A. Zuris, D.A. Halim, A.R. Conlan, E.C. Abresch, R. Nechushtai, M.L. Paddock, P.A. Jennings, Engineering the redox potential over a wide range within a new class of FeS proteins, J. Am. Chem. Soc. 132 (2010) 13120–13122.
[42] E.L. Baxter, J.A. Zuris, C. Wang, P.L. Vo, H.L. Axelrod, A.E. Cohen, M.L. Paddock, R. Nechushtai, J.N. Onuchic, P.A. Jennings, Allosteric control in a metalloprotein dramatically alters function, Proc. Natl. Acad. Sci. U. S. A. 110 (2013) 948–953.
[43] E.L. Baxter, P.A. Jennings, J.N. Onuchic, Interdomain communication revealed in the diabetes drug target mitoNEET, Proc. Natl. Acad. Sci. U. S. A. 108 (2011) 5266–5271.
[44] R. Nechushtai, H. Lammert, D. Michaeli, Y. Eisenberg-Domovich, J.A. Zuris, M.A. Luca, D.T. Capraro, A. Fish, O. Shimshon, M. Roy, A. Schug, P.C. Whitford, O. Livnah, J.N. Onuchic, P.A. Jennings, Allostery in the ferredoxin protein motif does not involve a conformational switch, Proc. Natl. Acad. Sci. U. S. A. 108 (2011) 2240–2245.
[45] Y. Shimomura, K. Wada, K. Fukuyama, Y. Takahashi, The asymmetric trimeric architecture of [2Fe–2S] IscU: implications for its scaffolding during iron–sulfur cluster biosynthesis, J. Mol. Biol. 383 (2008) 133–143.
[46] F. Bonomi, S. Iametti, D. Ta, L.E. Vickery, Multiple turnover transfer of [2Fe2S] clusters by the iron–sulfur cluster assembly scaffold proteins IscU and IscA, J. Biol. Chem. 280 (2005) 29513–29518.
[47] J.A. Zuris, Y. Harir, A.R. Conlan, M. Shvartsman, D. Michaeli, S. Tamir, M.L. Paddock, J.N. Onuchic, R. Mittler, Z.I. Cabantchik, P.A. Jennings, R. Nechushtai, Facile transfer of [2Fe–2S] clusters from the diabetes drug target mitoNEET to an apo-acceptor protein, Proc. Natl. Acad. Sci. U. S. A. 108 (2011) 13047–13052.
[48] F. Petrat, H. de Groot, R. Sustmann, U. Rauen, The chelatable iron pool in living cells: a methodically defined quantity, Biol. Chem. 383 (2002) 489–502.
[49] M. Shvartsman, Z. Ioav Cabantchik, Intracellular iron trafficking: role of cytosolic ligands, Biometals 25 (2012) 711–723.
[50] Z.I. Cabantchik, Labile iron in cells and body fluids: physiology, pathology, and pharmacology, Front. Pharmacol. 5 (2014) 45.
[51] Y.S. Sohn, S. Tamir, L. Song, D. Michaeli, I. Matouk, A.R. Conlan, Y. Harir, S.H. Holt, V. Shulaev, M.L. Paddock, A. Hochberg, I.Z. Cabanchick, J.N. Onuchic, P.A. Jennings, R. Nechushtai, R. Mittler, NAF-1 and mitoNEET are central to human breast cancer proliferation by maintaining mitochondrial homeostasis and promoting tumor growth, Proc. Natl. Acad. Sci. U. S. A. 110 (2013) 14676–14681.
[52] B. Levine, D.J. Klionsky, Development by self-digestion: molecular mechanisms and biological functions of autophagy, Dev. Cell 6 (2004) 463–477.
[53] M. Su, Y. Mei, S. Sinha, Role of the crosstalk between autophagy and apoptosis in cancer, J. Oncol. 2013 (2013) 102735.
[54] N.C. Chang, M. Nguyen, J. Bourdon, P.A. Risse, J. Martin, G. Danialou, R. Rizzuto, B.J. Petrof, G.C. Shore, Bcl-2-associated autophagy regulator Naf-1 required for maintenance of skeletal muscle, Hum. Mol. Genet. 21 (2012) 2277–2287.
[55] N.C. Chang, M. Nguyen, M. Germain, G.C. Shore, Antagonism of Beclin 1-dependent autophagy by BCL-2 at the endoplasmic reticulum requires NAF-1, EMBO J. 29 (2010) 606–618.
[56] N.C. Chang, M. Nguyen, G.C. Shore, BCL2–CISD2: an ER complex at the nexus of autophagy and calcium homeostasis? Autophagy 8 (2012) 856–857.
[57] M.C. Maiuri, A. Criollo, G. Kroemer, Crosstalk between apoptosis and autophagy within the Beclin 1 interactome, EMBO J. 29 (2010) 515–516.
[58] S. Tamir, S. Rotem-Bamberger, C. Katz, F. Morcos, K.L. Hailey, J.A. Zuris, C. Wang, A.R. Conlan, C.H. Lipper, M.L. Paddock, R. Mittler, J.N. Onuchic, P.A. Jennings, A. Friedler, R. Nechushtai, Integrated strategy reveals the protein interface between cancer targets Bcl-2 and NAF-1, Proc. Natl. Acad. Sci. U. S. A. 111 (2014) 5177–5182.
[59] L.W. Su, S.H. Chang, M.Y. Li, H.Y. Huang, W.N. Jane, J.Y. Yang, Purification and biochemical characterization of *Arabidopsis* At-NEET, an ancient iron–sulfur protein, reveals a conserved cleavage motif for subcellular localization, Plant Sci. 213 (2013) 46–54.
[60] A.P. Landry, H. Ding, Redox control of human mitochondrial outer membrane protein mitoNEET [2Fe–2S] clusters by biological thiols and hydrogen peroxide, J. Biol. Chem. 289 (2014) 4307–4315.
[61] M.E. Roberts, J.P. Crail, M.M. Laffoon, W.G. Fernandez, M.A. Menze, M.E. Konkle, Identification of disulfide bond formation between mitoNEET and glutamate dehydrogenase 1, Biochemistry 52 (2013) 8969–8971.
[62] J.R. Colca, R.F. Kletzien, What has prevented the expansion of insulin sensitisers? Expert Opin. Investig. Drugs 15 (2006) 205–210.
[63] C.W. Bolten, P.M. Blanner, W.G. McDonald, N.R. Staten, R.A. Mazzarella, G.B. Arhancet, M.F. Meier, D.J. Weiss, P.M. Sullivan, A.E. Hromockyj, R.F. Kletzien, J.R. Colca, Insulin sensitizing pharmacology of thiazolidinediones correlates with mitochondrial gene expression rather than activation of PPAR gamma, Gene Regul. Syst. Bio. 1 (2007) 73–82.

[64] R.L. Hunter, D.Y. Choi, S.A. Ross, G. Bing, Protective properties afforded by pioglitazone against intrastriatal LPS in Sprague–Dawley rats, Neurosci. Lett. 432 (2008) 198–201.
[65] W.J. Geldenhuys, M.O. Funk, K.F. Barnes, R.T. Carroll, Structure-based design of a thiazolidinedione which targets the mitochondrial protein mitoNEET, Bioorg. Med. Chem. Lett. 20 (2010) 819–823.
[66] R.M. Bieganski, M.L. Yarmush, Novel ligands that target the mitochondrial membrane protein mitoNEET, J. Mol. Graph. Model. 29 (2011) 965–973.
[67] W. Arif, S. Xu, D. Isailovic, W.J. Geldenhuys, R.T. Carroll, M.O. Funk, Complexes of the outer mitochondrial membrane protein mitoNEET with resveratrol-3-sulfate, Biochemistry 50 (2011) 5806–5811.
[68] W.J. Geldenhuys, M.O. Funk, P.S. Awale, L. Lin, R.T. Carroll, A novel binding assay identifies high affinity ligands to the rosiglitazone binding site of mitoNEET, Bioorg. Med. Chem. Lett. 21 (2011) 5498–5501.
[69] J.A. Zuris, S.S. Ali, H. Yeh, T.A. Nguyen, R. Nechushtai, M.L. Paddock, P.A. Jennings, NADPH inhibits [2Fe–2S] cluster protein transfer from diabetes drug target mitoNEET to an apo-acceptor protein, J. Biol. Chem. 287 (2012) 11649–11655.
[70] G. Tan, A.P. Landry, R. Dai, L. Wang, J. Lu, H. Ding, Competition of zinc ion for the [2Fe–2S] cluster binding site in the diabetes drug target protein mitoNEET, Biometals 25 (2012) 1177–1184.
[71] Z. Chen, P.A. Vigueira, K.T. Chambers, A.M. Hall, M.S. Mitra, N. Qi, W.G. McDonald, J.R. Colca, R.F. Kletzien, B.N. Finck, Insulin resistance and metabolic derangements in obese mice are ameliorated by a novel peroxisome proliferator-activated receptor gamma-sparing thiazolidinedione, J. Biol. Chem. 287 (2012) 23537–23548.
[72] D.L. Feinstein, A. Spagnolo, C. Akar, G. Weinberg, P. Murphy, V. Gavrilyuk, C. Dello Russo, Receptor-independent actions of PPAR thiazolidinedione agonists: is mitochondrial function the key? Biochem. Pharmacol. 70 (2005) 177–188.
[73] C.M. Kusminski, W.L. Holland, K. Sun, J. Park, S.B. Spurgin, Y. Lin, G.R. Askew, J.A. Simcox, D.A. McClain, C. Li, P.E. Scherer, MitoNEET-driven alterations in adipocyte mitochondrial activity reveal a crucial adaptive process that preserves insulin sensitivity in obesity, Nat. Med. 18 (2012) 1539–1549.
[74] N. Shulga, J.G. Pastorino, Mitoneet mediates TNFα induced necroptosis promoted by fructose and ethanol exposure, J. Cell Sci. 127 (2014) 896–907.
[75] J.R. Colca, Insulin sensitizers may prevent metabolic inflammation, Biochem. Pharmacol. 72 (2006) 125–131.
[76] R. Stark, M. Roden, E.S.C.I. Award, Mitochondrial function and endocrine diseases, Eur. J. Clin. Invest. 37 (2007) (2006) 236–248.
[77] P. Bandyopadhyay, Novel therapies in diabetes mellitus, Drug News Perspect. 19 (2006) 499–507.
[78] I. Bogacka, H. Xie, G.A. Bray, S.R. Smith, Pioglitazone induces mitochondrial biogenesis in human subcutaneous adipose tissue *in vivo*, Diabetes 54 (2005) 1392–1399.
[79] B. Brunmair, K. Staniek, F. Gras, N. Scharf, A. Althaym, R. Clara, M. Roden, E. Gnaiger, H. Nohl, W. Waldhausl, C. Furnsinn, Thiazolidinediones, like metformin, inhibit respiratory complex I: a common mechanism contributing to their antidiabetic actions? Diabetes 53 (2004) 1052–1059.
[80] W.J. Geldenhuys, T.C. Leeper, R.T. Carroll, mitoNEET as novel drug target for mitochondrial dysfunction, Drug Discov. Today 19 (2014) 1601–1606.
[81] W.J. Geldenhuys, C.J. Van der Schyf, Rationally designed multi-targeted agents against neurodegenerative diseases, Curr. Med. Chem. 20 (2013) 1662–1672.
[82] T. Zhou, J. Lin, Y. Feng, J. Wang, Binding of reduced nicotinamide adenine dinucleotide phosphate destabilizes the iron–sulfur clusters of human mitoNEET, Biochemistry 49 (2010) 9604–9612.
[83] G.L. Taminelli, V. Sotomayor, A.G. Valdivieso, M.L. Teiber, M.C. Marin, T.A. Santa-Coloma, *CISD1* codifies a mitochondrial protein upregulated by the *CFTR* channel, Biochem. Biophys. Res. Commun. 365 (2008) 856–862.
[84] K. Okatsu, S. Iemura, F. Koyano, E. Go, M. Kimura, T. Natsume, K. Tanaka, N. Matsuda, Mitochondrial hexokinase HKI is a novel substrate of the Parkin ubiquitin ligase, Biochem. Biophys. Res. Commun. 428 (2012) 197–202.
[85] R.K. Kaundal, S.S. Sharma, Peroxisome proliferator-activated receptor gamma agonists as neuroprotective agents, Drug News Perspect. 23 (2010) 241–256.
[86] H.M. Yonutas, P.G. Sullivan, Targeting PPAR isoforms following CNS injury, Curr. Drug Targets 14 (2013) 733–742.
[87] Y.F. Chen, C.Y. Wu, R. Kirby, C.H. Kao, T.F. Tsai, A role for the CISD2 gene in lifespan control and human disease, Ann. N. Y. Acad. Sci. 1201 (2010) 58–64.
[88] M.A. Jones, S. Amr, A. Ferebee, P. Huynh, J.A. Rosenfeld, M.F. Miles, A.G. Davies, C.A. Korey, J.M. Warrick, R. Shiang, S.H. Elsea, S. Girirajan, M. Grotewiel, Genetic studies in *Drosophila* and humans support a model for the concerted function of *CISD2*, *PPT1* and *CLN3* in disease, Biol. Open 3 (2014) 342–352.
[89] C.Y. Wu, Y.F. Chen, C.H. Wang, C.H. Kao, H.W. Zhuang, C.C. Chen, L.K. Chen, R. Kirby, Y.H. Wei, S.F. Tsai, T.F. Tsai, A persistent level of Cisd2 extends healthy lifespan and delays aging in mice, Hum. Mol. Genet. 21 (2012) 3956–3968.
[90] G. Stelzer, I. Dalah, T.I. Stein, Y. Satanower, N. Rosen, N. Nativ, D. Oz-Levi, T. Olender, F. Belinky, I. Bahir, H. Krug, P. Perco, B. Mayer, E. Kolker, M. Safran, D. Lancet, *In-silico* human genomics with GeneCards, Hum. Genom. 5 (2011) 709–717.
[91] http://www.genecards.org/cgi-bin/carddisp.pl?gene=CISD1, CISD2.
[92] D.F. Cortes, W. Sha, V. Hower, G. Blekherman, R. Laubenbacher, S. Akman, S.V. Torti, V. Shulaev, Differential gene expression in normal and transformed human mammary epithelial cells in response to oxidative stress, Free Radic. Biol. Med. 50 (2011) 1565–1574.
[93] A.F. Salem, D. Whitaker-Menezes, A. Howell, F. Sotgia, M.P. Lisanti, Mitochondrial biogenesis in epithelial cancer cells promotes breast cancer tumor growth and confers autophagy resistance, Cell Cycle 11 (2012) 4174–4180.
[94] C. Katz, H. Benyamini, S. Rotem, M. Lebendiker, T. Danieli, A. Iosub, H. Refaely, M. Dines, V. Bronner, T. Bravman, D.E. Shalev, S. Rudiger, A. Friedler, Molecular basis of the interaction between the antiapoptotic Bcl-2 family proteins and the proapoptotic protein ASPP2, Proc. Natl. Acad. Sci. U. S. A. 105 (2008) 12277–12282.
[95] C. Katz, L. Levy-Beladev, S. Rotem-Bamberger, T. Rito, S.G. Rüdiger, A. Friedler, Studying protein–protein interactions using peptide arrays, Chem. Soc. Rev. 40 (2011) 2131–2145.
[96] Z. Wang, M. Gerstein, M. Snyder, RNA-Seq: a revolutionary tool for transcriptomics, Nat. Rev. Genet. 10 (2009) 57–63.
[97] P.A. McGettigan, Transcriptomics in the RNA-seq era, Curr. Opin. Chem. Biol. 17 (2013) 4–11.
[98] S. Bhattacharya, T.J. Mariani, Systems biology approaches to identify developmental bases for lung diseases, Pediatr. Res. 73 (2013) 514–522.
[99] V. Costa, M. Aprile, R. Esposito, A. Ciccodicola, RNA-Seq and human complex diseases: recent accomplishments and future perspectives, Eur. J. Hum. Genet. 21 (2013) 134–142.
[100] T. Kavanagh, J.D. Mills, W.S. Kim, G.M. Halliday, M. Janitz, Pathway analysis of the human brain transcriptome in disease, J. Mol. Neurosci. 51 (2013) 28–36.
[101] N.E. Babady, N. Carelle, R.D. Wells, T.A. Rouault, M. Hirano, D.R. Lynch, M.B. Delatycki, R.B. Wilson, G. Isaya, H. Puccio, Advancements in the pathophysiology of Friedreich's ataxia and new prospects for treatments, Mol. Genet. Metab. 92 (2007) 23–35.
[102] G. Blekherman, R. Laubenbacher, D.F. Cortes, P. Mendes, F.M. Torti, S. Akman, S.V. Torti, V. Shulaev, Bioinformatics tools for cancer metabolomics, Metabolomics 7 (2011) 329–343.
[103] L. Denoroy, L. Zimmer, B. Renaud, S. Parrot, Ultra high performance liquid chromatography as a tool for the discovery and the analysis of biomarkers of diseases: a review, J. Chromatogr. B Anal. Technol. Biomed. Life Sci. 927 (2013) 37–53.
[104] H. Lv, Mass spectrometry-based metabolomics towards understanding of gene functions with a diversity of biological contexts, Mass Spectrom. Rev. 32 (2013) 118–128.
[105] D. Nagrath, C. Caneba, T. Karedath, N. Bellance, Metabolomics for mitochondrial and cancer studies, Biochim. Biophys. Acta 1807 (2011) 650–663.
[106] D.S. Wishart, D. Tzur, C. Knox, R. Eisner, A.C. Guo, N. Young, D. Cheng, K. Jewell, D. Arndt, S. Sawhney, C. Fung, L. Nikolai, M. Lewis, M.A. Coutouly, I. Forsythe, P. Tang, S. Shrivastava, K. Jeroncic, P. Stothard, G. Amegbey, D. Block, D.D. Hau, J. Wagner, J. Miniaci, M. Clements, M. Gebremedhin, N. Guo, Y. Zhang, G.E. Duggan, G.D. Macinnis, A.M. Weljie, R. Dowlatabadi, F. Bamforth, D. Clive, R. Greiner, L. Li, T. Marrie, B.D. Sykes, H.J. Vogel, L. Querengesser, HMDB: the Human Metabolome Database, Nucleic Acids Res. 35 (2007) D521–D526.
[107] F. Morcos, A. Pagnani, B. Lunt, A. Bertolino, D.S. Marks, C. Sander, R. Zecchina, J.N. Onuchic, T. Hwa, M. Weigt, Direct-coupling analysis of residue coevolution captures native contacts across many protein families, Proc. Natl. Acad. Sci. U. S. A. 108 (2011) E1293–E1301.
[108] J.I. Sulkowska, F. Morcos, M. Weigt, T. Hwa, J.N. Onuchic, Genomics-aided structure prediction, Proc. Natl. Acad. Sci. U. S. A. 109 (2012) 10340–10345.
[109] D.S. Marks, L.J. Colwell, R. Sheridan, T.A. Hopf, A. Pagnani, R. Zecchina, C. Sander, Protein 3D structure computed from evolutionary sequence variation, PLoS ONE 6 (2011) e28766.
[110] B. Jana, F. Morcos, J.N. Onuchic, From structure to function: the convergence of structure based models and co-evolutionary information, Phys. chem. chem. phys.: PCCP 16 (2014) 6496–6507.
[111] F. Morcos, B. Jana, T. Hwa, J.N. Onuchic, Coevolutionary signals across protein lineages help capture multiple protein conformations, Proc. Natl. Acad. Sci. U. S. A. 110 (2013) 20533–20538.
[112] A. Schug, M. Weigt, J.N. Onuchic, T. Hwa, H. Szurmant, High-resolution protein complexes from integrating genomic information with molecular simulation, Proc. Natl. Acad. Sci. U. S. A. 106 (2009) 22124–22129.
[113] R.R. Cheng, F. Morcos, H. Levine, J.N. Onuchic, Toward rationally redesigning bacterial two-component signaling systems using coevolutionary information, Proc. Natl. Acad. Sci. U. S. A. 111 (2014) E563–E571.
[114] J.K. Noel, P.C. Whitford, K.Y. Sanbonmatsu, J.N. Onuchic, SMOG@ctbp: simplified deployment of structure-based models in GROMACS, Nucleic Acids Res. 38 (2010) W657–W661.
[115] C. Clementi, S.S. Plotkin, The effects of nonnative interactions on protein folding rates: theory and simulation, Protein Sci. 13 (2004) 1750–1766.
[116] I. Ferecatu, S. Gon alves, M.P. Golinelli-Cohen, M. Clémancey, A. Martelli, S. Riquier, E. Guittet, J.M. Latour, H. Puccio, J.C. Drapier, E. Lescop, C. Bouton, The diabetes drug target mitoNEET governs a novel trafficking pathway to rebuild an Fe–S cluster into cytosolic aconitase/iron regulatory protein 1, J. Biol. Chem. 289 (2014) 28070–28086.
[117] http://cluspro.bu.edu/queue.php.